

DTIC FILE COPY

AD-A219 319		ON PAGE	Form Approved OMB No. 0704-0188
Public Reproduction Collection Data High		1. How best response, including the time for reviewing information, searching existing data sources, collection of information, send comments regarding this burden estimate or any other aspect of this collection of information, including suggestions for reducing this burden, to Washington Headquarters Services, Directorate for Information Operations and Reports, 1215 Jefferson Avenue, Washington, DC 20540.	
1. AGE	1989/10/30	2. REPORT TYPE AND DATES COVERED INTERIM 11/1/88 to 10/30/89	
4. TITLE AND SUBTITLE Visual sensitivities and discriminations and their role in aviation		5. FUNDING NUMBERS F49620-88-C0002	
6. AUTHOR(S) David Regan, Ph.D., D.Sc., F.R.S.C.			
7. PERFORMING ORGANIZATION NAME(S) AND ADDRESS(ES) York University, (Mrs. N. Swatman) Rm. S415 Ross Bldg., York University, 4700 Keele Street, North York, Ontario, Canada M3J 1P3		8. PERFORMING ORGANIZATION REPORT NUMBER 61102F 2313/A5	
9. SPONSORING/MONITORING AGENCY NAME(S) AND ADDRESS(ES) AFOSR Life Sciences Directorate Bolling AFB DC 20332		10. SPONSORING/MONITORING AGENCY REPORT NUMBER 90-0235 AFOSR-TR DL	
11. SUPPLEMENTARY NOTES			
12a. DISTRIBUTION/AVAILABILITY STATEMENT unlimited		12b. DISTRIBUTION CODE DTIC S ELECTE FEB 26 1990 B D	
13. ABSTRACT (Maximum 200 words) (1) Selective "blindness" to approaching or receding motion in depth exists and seems to be not uncommon in normally-sighted individuals. Of 16 subjects, 8 had visual field defects for either approaching or receding motion. Of 21 subjects, only 6 had full symmetrical fields for oscillatory motion in depth. Visual sensitivity to sideways motion was normal in stereomotion-blind areas. The possible relevance to aviation is pointed out. (2) A perfectly camouflaged bar within a random dot pattern was rendered visible by moving dots within the bar and outside the bar with equal and opposite velocities (motion parallax). The bar's orientation could be judged with equal precision (0.5 deg) to that of an uncamouflaged dotted bar made visible by brightness contrast providing that dot speed and contrast were high. But when contrast was reduced, discrimination collapsed for the camouflaged bar (3) Shape discrimination was compared for motion-defined and contrast-defined dotted rectangles. At high dot speeds and contrasts aspect ratio discrimination equal for the two kinds of rectangle and, at 2-3%, corresponded to a change of side length of only 24 arc sec. (4) Orientation discrimination and shape discrimination degrade more rapidly at short presentation durations for a motion-defined than for a contrast-defined target. (5) The findings in (2) - (4) above suggest that helicopter pilots may be at risk of			
14. SUBJECT TERMS vision; visual flying skills; visual assessment; stereo; motion perception; evoked potentials; neuromagnetic recording; nonlinear analysis		15. NUMBER OF PAGES 67	
17. SECURITY CLASSIFICATION OF REPORT Unclassified		18. SECURITY CLASSIFICATION OF THIS PAGE Unclassified	
19. SECURITY CLASSIFICATION OF ABSTRACT Unclassified		20. LIMITATION OF ABSTRACT	

making visual judgement errors in nap of the earth flight where some objects and ground features are seen by motion alone when contrast or speed is low or when inspection duration is brief. (6) We have developed a simple portable test for assessing visual ability to see and discriminate motion-defined form. It is a letter reading test suitable for field use and for medical use. (7) The motion-defined letter test was used on 25 patients with multiple sclerosis and 50 controls; 34/50 eyes of patients were abnormal even though visual acuity was normal. (8) Nonlinear systems analysis: We have developed a new mathematical approach to testing multi-neuron models in which individuals neurons are modelled as rectifiers. (9) We have developed a nondestructive zoom-FFT technique that allows spectra of EEG and other time series to be computed with the theoretical resolution allowed by the Heisenberg-Gabor relation, e.g. 50,000 lines DC-100 Hz at a resolution of 0.002 Hz from a 500-sec recording. (10) By using a 2-sinewave nonlinear analysis approach in recording human evoked potentials we have found that both vertically-tuned and horizontally-tuned responses have a bandwidth of about 12 deg, and that there is a strong nonlinear interaction between horizontal and vertical. (11) Single-cell responses: We have built electronics to allow single cell recordings to be analyzed, and carried out pilot experiments. (12) A magnetically-shielded room, 7-channel magnetometer and sensory position indicator (SPI) have been installed at York University and several faults rectified. We have investigated nonlinearities in the response to two visual stimuli of different frequencies and two auditory stimuli of different frequencies, analyzing the responses by zoom-FFT. (13) A book "Human Brain Electrophysiology" written by the P.I. was published in 1989. (14) Two books edited by the P.I., one on "Binocular Vision" and one on "Spatial Vision" are in press for 1990 publication.

Accession For	
NTIS GRA&I	<input checked="checked" type="checkbox"/>
DTIC TAB	<input type="checkbox"/>
Unannounced	<input type="checkbox"/>
Justification	
By	
Distribution/	
Availability Codes	
Dist	Avail and/or Special
A-1	



2a. Objectives: Psychophysical

(1) Further define the roles of the channeling hypothesis in: (a) identifying specific visual processes; (b) understanding visual performance; (c) specifying visual parameters likely to be important in eye-hand coordination, especially in aviation and flight simulator visual displays.

(2) *Camouflage and the visual processing of objects defined by motion alone.* For camouflaged objects that are invisible except when there is motion parallax between the object and background, measure spatial discriminations, and in particular the hyperacuties, orientation discrimination, spatial frequency discrimination, and line interval discrimination. Compare these data with the corresponding hyperacuties for objects defined by luminance contrast, and find whether both sets of data can be explained by an opponent or line-element model of spatial form discrimination proposed previously.⁽¹⁻⁵⁾

2a. Objectives: Neuromagnetism and electrophysiology

(1) Link the channeling modes of human psychophysics with the activation of different sensory projection areas in human cortex.

(2) Identify evoked activity in different visual, auditory or somatosensory projections in human cortex and elucidate the differences between the type of processing occurring in the different areas. Link these data with the known functional neuroanatomy of macaque monkey brain and with human psychophysics.

(3) Elucidate the temporal sequence of activation of different cortical areas evoked by different kinds of complex visual auditory and somatosensory stimuli. These data will complement scanning data (e.g. regional cerebral blood flow, PET) that lack the temporal resolution offered by neuromagnetic recording.



- (4) Elucidate relationships between simultaneous activities of different cortical areas within a single modality (visual, auditory or somatosensory).
- (5) Identify the cortical sites of interactions between responses to stimuli of different modalities, and compare these sites with the known poly-sensory cortical areas in nonhuman primates.
- (6) By combining neuromagnetic and evoked potential recording, exploit their complementary natures to improve the localization of generator sites.
- (7) Locate the brain sites of abnormalities in patients with known specific sensory defects including selective orientation-tuned visual loss for intermediate spatial frequencies, stereomotion "blindness", specific defects of shape recognition, selective deafness to frequency changes.

2b. Status of the Research Effort: Psychophysical

- (1) *Specific "blindness" to oscillatory and unidirectional motion in depth.*

As an object moves towards the head its two retinal images move in opposite directions. This binocular cue alone can generate a strong impression of motion in depth (stereomotion). We have previously published visual fields for oscillatory motion in depth and found that normally-sighted subjects have areas of specific blindness to stereomotion.^(6,7) Of the six subjects reported, five showed stereomotion field defects. We have now extended the data base to a further 21 normal subjects, and confirm that stereomotion field defects are common. Only 6/21 subjects had full symmetrical fields.

We now report the existence of selective blindness to unidirectional motion in depth. Of 16 subjects whose visual fields were tested for approaching and for receding motion in depth, only 5 had similar fields for approaching and receding motion.



Table 1 summarizes the data. Figure 1 illustrates stereomotion fields that were full and symmetrical. Figure 2 shows fields for a subject with field defects and areas that were "blind" to motion in one direction.

Because sensitivity to monocularly-viewed motion showed no abnormalities corresponding to the binocular stereomotion "blind spots" we conclude that the stereomotion field defects were chiefly due to the *cortical* processing of motion. We also conclude that unidirectional motion defects are caused by a loss of sensitivity to unidirectional motion in depth rather than to abnormal interactions between mechanisms for approaching and receding motion. These findings provide further evidence that the human visual pathway contains different binocular mechanisms for position in depth and for motion in depth, and that stereomotion blindness is due to a selective loss of the motion mechanism.

These findings raise the possibility that stereomotion "blind spots" are not uncommon in pilots, and that the trajectory of an oncoming aircraft might be misjudged if it passed through a stereomotion "blind spot".

A report on the results to date has been published in *Vision Research*.⁽⁸⁾

(2) *Orientation discrimination for camouflaged objects defined by motion alone and for objects defined by luminance contrast*

A pseudo-random pattern of bright dots subtending 2.2×2.2 deg was generated by hardware of our own design. Frame rate was 200 Hz. Dots subtended 2.0 min arc, mean separation was about 6 min arc and there were approximately 1000 dots. The dots were optically superimposed on a circular uniformly-illuminated area of diameter 3.7 deg. A 1.5×0.22 deg bar-



UNIVERSITÉ
YORK
UNIVERSITY

FACULTY OF ARTS

4700 KEELE STREET • NORTH YORK • ONTARIO • CANADA • M3J 1P3

**Table 1. Summary of results for 21 normally-sighted subjects. Key:
D- different fields. S - similar fields. U - unclassified. U(PR) -
unclassified with poor reproducibility.**

TABLE 1

SUBJECT	SINEWAVE FIELDS		RAMP FIELDS			
	LARGE	FAR / NEAR	FAR / NEAR		TOWARDS / AWAY	
			TOWARDS	AWAY	NEAR	FAR
1	-	D	U	U(PR)	U(PR)	S
2	-	D	D	D	D	U
3	-	D	U	S	D	U
4	-	D	S	S	S	S
5	-	D	S	D	S	D
6	-	D	S	D	D	S
7	-	D	D	D	S	U
8	-	S	U(PR)	U(PR)	U(PR)	U(PR)
9	-	S	S	S	S	S
10	X	S	S	S	S	S
11	X	U	U	S	D	S
12	-	U	D	S	D	S
13	-	S	S	S	S	S
14	-	S	S	U	U	S
15	X	S	S	S	S	S
16	X	S	-	-	-	-
17	-	S	-	-	-	-
18	X	S	-	-	-	-
19	-	S	-	-	-	-
20	X	S	-	-	-	-
21	-	D	U(PR)	D	U(PR)	U

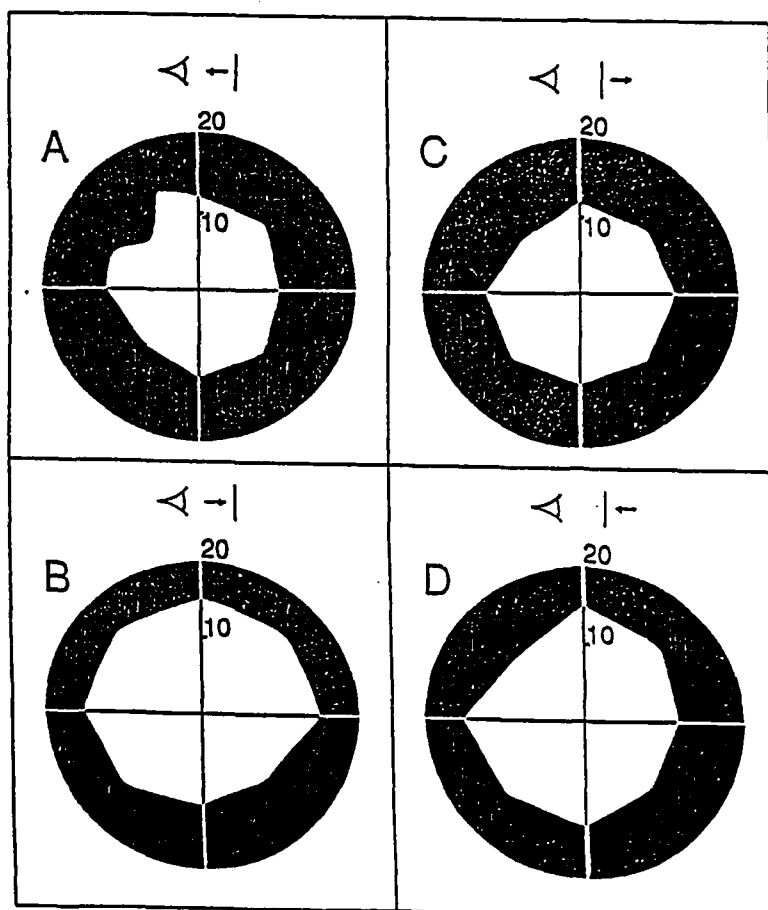


Figure 1. Visual fields for unidirectional depth perception.
A subject with similar large fields for approaching and receding motion.

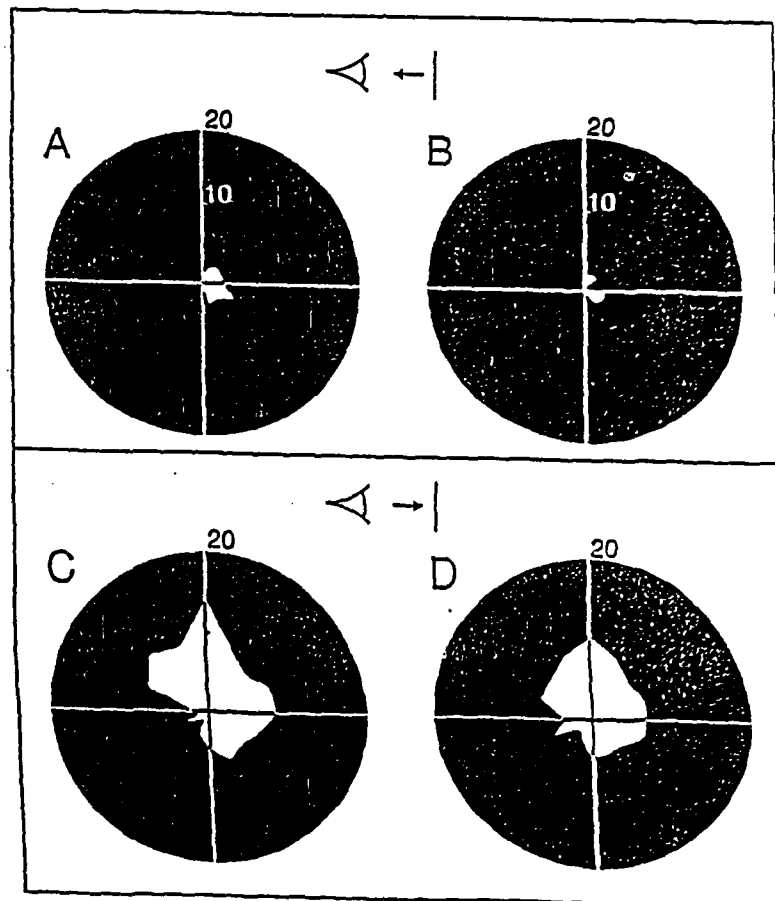


Figure 2. Large visual field defect for unidirectional depth perception. A, B; near disparities, approaching motion. C, D: near disparities, receding motion.



shaped area within the dot pattern was rendered visible by moving dots inside this area leftwards and outside this area rightwards at constant velocity. When the dots were stationary the bar was perfectly camouflaged. Dot contrast was varied by neutral density filters. Orientation discrimination was measured by temporal two-alternative forced choice. The dot pattern was presented for 1.0 sec, and contained a motion-defined vertical bar. Then there was an interval of 0.5 sec followed by a second presentation of 1.0 sec with the bar inclined at some angle θ . There were 10 possible values of θ . Bar location was randomly jittered and a fresh random dot pattern was generated for each presentation. The subject pressed one of two buttons depending on whether θ was clockwise or anticlockwise of vertical. Orientation discrimination threshold was calculated by Probit analysis.

In separate experiments orientation discrimination was measured for a non-camouflaged bar that was created by omitting the dots in the area surrounding the bar. This target is illustrated in Figure 3.

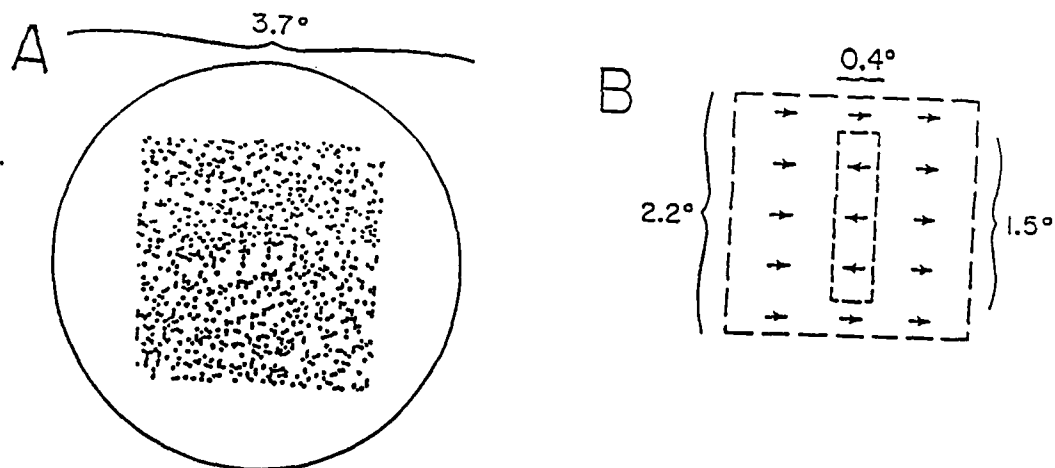


Figure 3. A - random dot pattern containing a perfectly camouflaged bar. B - the bar was revealed by moving dots within the bar and outside the bar in opposite directions.



The rationale of this experiment is that, for the camouflaged bar, figure ground segregation was achieved by motion alone but the non-camouflaged bar was rendered visible by luminance contrast. Dot density and velocity within the bar were identical in the two cases.

Figures 4 and 5 show that, for high dot velocities and contrasts, orientation discrimination is similar for motion-defined and contrast-defined bars. Furthermore, at about 0.4 deg, discrimination compares favourably with the most acute values reported in the literature for conventional bright solid bars or lines. This finding may relate to our previous finding that vernier acuity for a camouflaged dotted bar can be as high as for a non-camouflaged dotted bar (see Final Report dated 1987/09/14 and Reference #9).

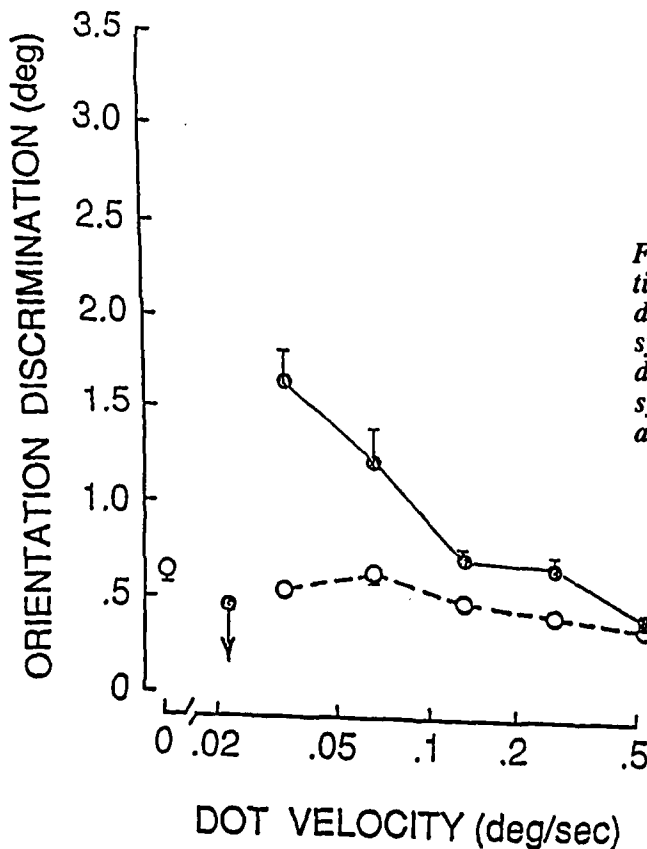


Figure 4. Orientation discrimination versus dot speed for a dotted bar defined by relative motion (open symbols) and for the same bar defined by luminance contrast (filled symbols). Bar detection thresholds are arrowed

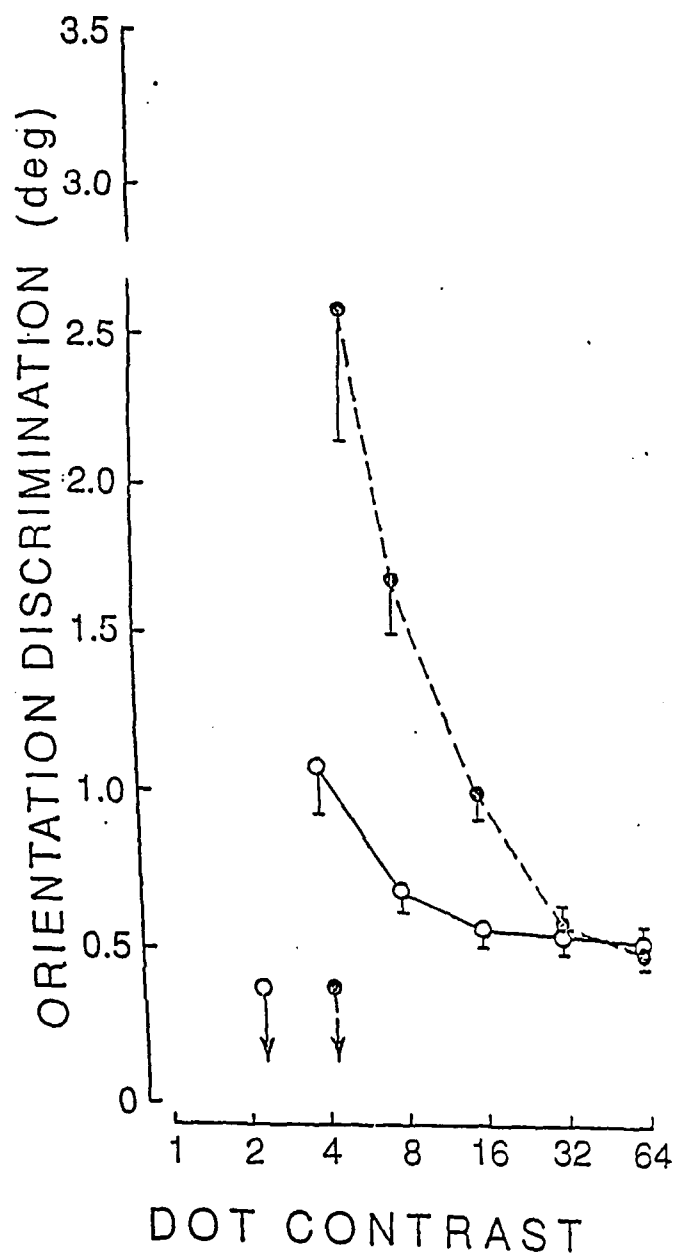


Figure 5. Orientation discrimination versus dot contrast. Other details as in Figure 4.



But Figure 5 also shows that, as contrast is reduced, discrimination collapses earlier for the motion-defined bar than for the contrast-defined bar. In particular, there is a contrast range of about 4:1 over which discrimination has collapsed for the motion-defined bar but is still good for the contrast-defined bar.

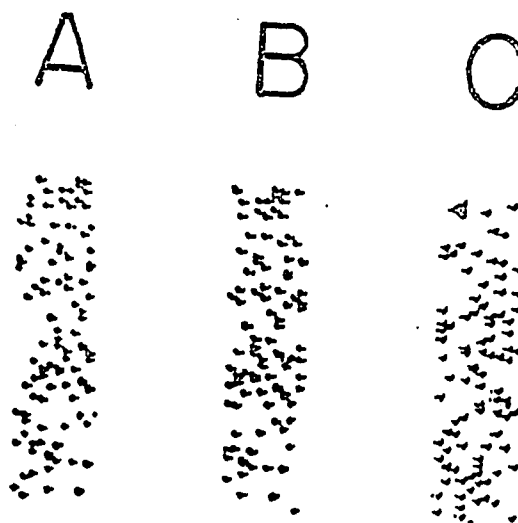


Figure 6. A-C are three snapshots of the dotted bar taken during a 1.0 sec presentation. The dots surrounding the bar were switched off.

Turning back to Figure 4, we now consider the effect of dot velocity on discrimination for the camouflaged motion-visible bar. It is, in principle, possible that dot motion might improve discrimination by reducing errors due to spatial sampling by dots. Figure 6 illustrates this point. Because of the coarse spatial sampling provided by the sparse dots, the orientation of the bar's edge is poorly defined in each photograph. But in principle, orientation could be more precisely defined by taking all three "snapshots" into account. However, Figure 4 shows that this effect did not occur for the contrast defined bar (filled symbols). We can therefore assume that the effect of velocity on discrimination for the camouflaged bar (open symbols) was due to velocity sensitivity of motion-sensitive mechanisms rather than to sampling errors.

A preliminary report of this study has been published in *Vision Research*.⁽¹⁰⁾

(3) *Shape discrimination for camouflaged objects defined by motion alone and for objects defined by luminance contrast*

We have used a similar technique to that described in #2 above to generate a camouflaged rectangular shape that is visible by motion alone. The rectangular area was rendered visible by moving the dots inside the rectangle obliquely downwards to the left at a constant speed that was equal and opposite to the speed of the dots in the remainder of the pattern. The reason for choosing oblique motion was to ensure that the rectangle's vertical and horizontal edges were all defined by the same mix of shearing and compressive motion. Although the rectangle was visible to the eye, a photographic time exposure did not reveal it (Figure 7B). Contrast-defined rectangles were created by switching off all dots outside the rectangle (Figure 7C). The ratio between the lengths of vertical and horizontal sides had 10 possible values, and these were presented randomly. The subject's task was to press one of two buttons depending on whether the longer sides were

vertical or horizontal. To ensure that both dimensions must be compared, different areas of rectangle were interleaved randomly as illustrated in Figure 8. To ensure that the distance of any edge from the boundary of the display provides no cue to shape, the rectangle's location was jittered randomly. Shape discrimination threshold was measured by two-alternative forced choice and Probit analysis.

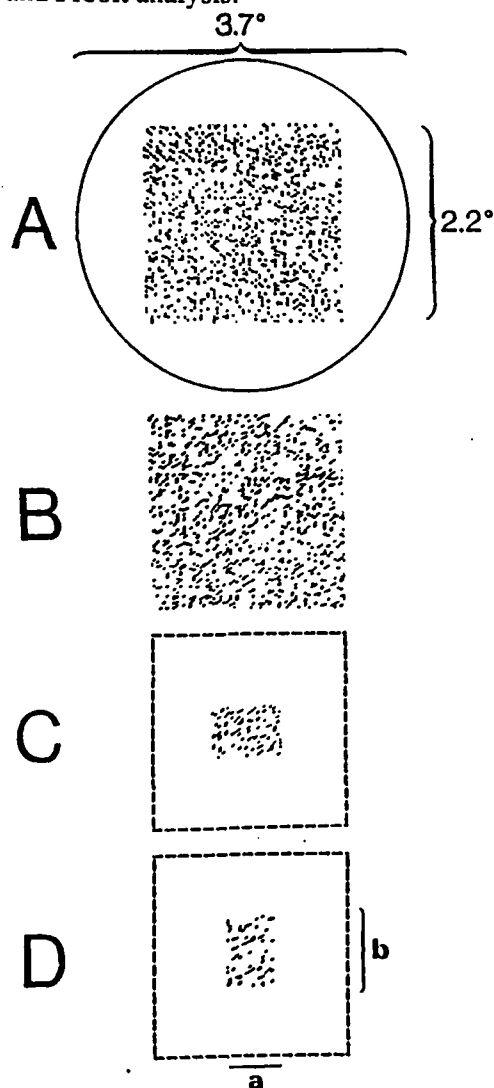


Figure 7. A- Photograph of a typical random dot pattern. The test rectangle is perfectly camouflaged. The outer circle marks the edge of the superimposed adapting field. B- Dots within the rectangle and outside the rectangle were moved at equal and opposite speeds. Although the rectangle was evident to the eye, it was not evident to the camera. C- All dots outside the rectangle were switched off to create an uncamouflaged rectangle. Aspect ratio was defined as (a/b) .



DISSOCIATION OF ASPECT RATIO (a/b) FROM LINEAR DIMENSIONS

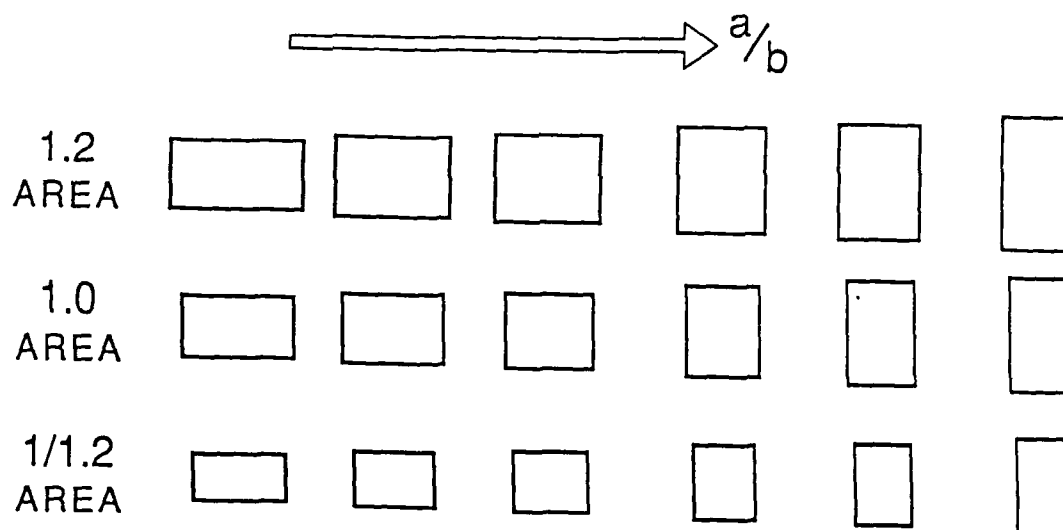


Figure 8. Dissociation of aspect ratio (a/b) from area and from any given linear dimension

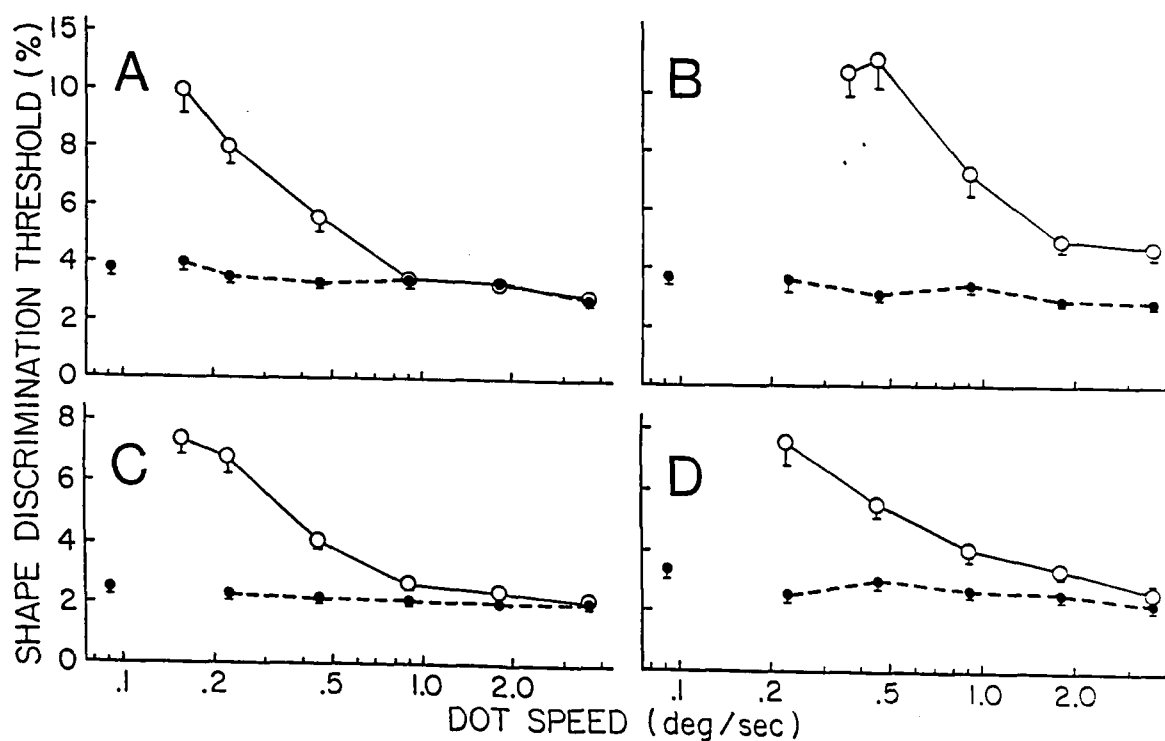


Figure 9. Ordinate plot shape discrimination thresholds $\Delta(a/b)$ expressed as a percentage, where $\Delta(a/b)$ is the smallest discriminable change in the ratio $\Delta(a/b)$. Abscissae plot dot speed (relative speed is twice dot speed). Open circles are for motion-defined rectangles and filled circles are for uncamouflaged rectangles. Dot contrast in B and D was 0.6 log units less than in A and C. The leftmost filled circles in each panel is for zero speed. A, B - subject 1. C, D - subject 2. Viewing was monocular.



We have measured shape discrimination as a function of dot speed and dot contrast for camouflaged dotted rectangles and for uncamouflaged dotted rectangles. Figure 9 shows that, when dot speed and contrast were both high, aspect ratio discrimination threshold was as acute for a motion-defined rectangle as for a contrast-defined rectangle and, at 2-3%, corresponded to a change of side length of about 24 arc sec. This is a remarkable visual performance, given that the mean dot separation was about 360 arc sec. Discrimination collapsed at low dot speeds and could not be measured at speeds less than about 0.1-0.2 deg/sec for motion-defined rectangles, but was almost unaffected by dot speed for contrast-defined rectangles. To explain how the visual system can dissociate changes of shape from changes of area we invoke a previous suggestion⁽¹¹⁾ that the visual system contains a mechanism that compares the separation of pairs of contours along perpendicular azimuths. To explain the coincidence of shape discrimination thresholds for motion-defined and contrast-defined rectangles we suggest, that in early visual development the underlying neural mechanisms are driven by the same environmental and behavioural pressures towards a common endpoint. In other words, "spatial vision is spatial vision" and the performance required for eye-hand coordination that is dictated by the outside environment independently of how the eye segregates figure from ground. This idea could also explain why orientation discrimination is the same for motion-defined and contrast-defined bars.

A report on this work has been submitted for publication⁽¹²⁾.

- (4) *Dynamics of orientation discrimination and shape discrimination for objects defined by motion along and for objects defined by luminance contrast*



We have studied the dynamics of orientation discrimination and shape discrimination in the following two ways: (A) By measuring discrimination threshold as a function of presentation duration, dot lifetime being equal to presentation duration; (B) by measuring discrimination threshold as a function of dot lifetime for a fixed presentation duration. These two studies are in progress. Results to date are as follows.

Figure 10 shows that, for presentation durations shorter than about 0.15 sec, shape discrimination rapidly became poorer for MD than for CD rectangles. This effect could not be attributed entirely to an elevation of simple motion detection threshold at low durations because the effect of duration on motion threshold (Figure 10B) was quite different to the effect of duration on shape discrimination (Figure 10A). In terms of a Reichardt-type model of figure-ground discrimination we might regard Figure 10B as reflecting the properties of peripheral motion detectors, and Figure 10B as reflecting the properties of figure-ground extraction and more central processing. In these terms, the difference curve (Figure 10C) reflects the properties of figure-ground extraction and more central processing.

The effect of presentation duration on orientation discrimination is similar to the effect on shape discrimination shown in Figure 10A. The effect of dot lifetime on orientation discrimination is somewhat different. Discrimination improves with dot lifetime up to about 100 msec, beyond which it has little effect.

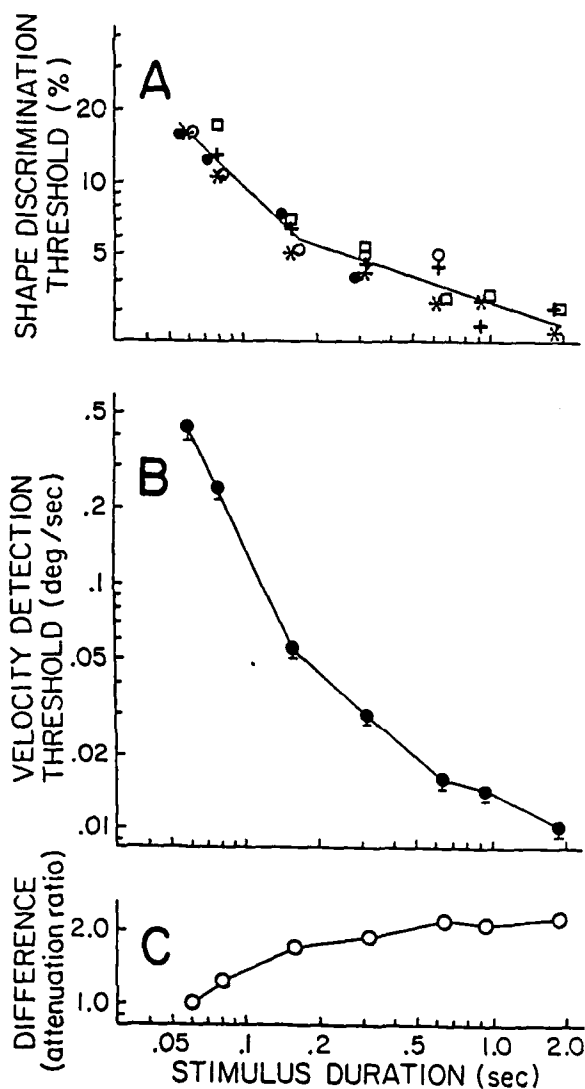


Figure 10. A- The effect of presentation duration on shape discrimination for camouflaged motion-defined rectangles. Just-discriminable differences in aspect ratio (ordinate) are plotted versus duration (abscissa) for 5 different dot speeds. Open square, plusses, filled stars, open circles, and filled circles respectively plot dot speeds of 0.18, 0.36, 0.68, 1.36 and 2.72 deg/sec. Aspect ratio is defined in Fig. 1D. The velocity difference between dots in the rectangle and surround equals twice the dot speed. B- The effect of presentation duration (abscissa) on velocity direction discrimination threshold defined as the lowest dot speed for which leftward and rightward motion could be discriminated with 75% accuracy. Both axes are logarithmic in A and B. C- Difference between the curves in A and B. Subject #1.

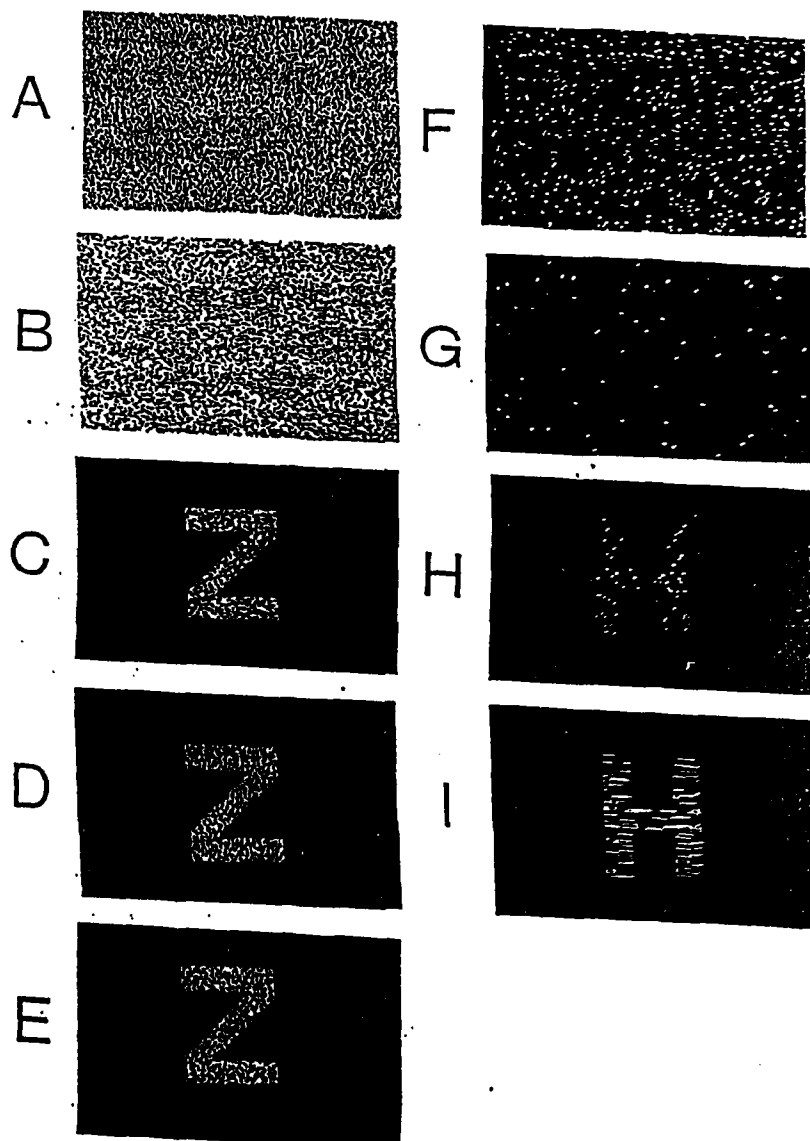


Figure 11 A- photograph of a typical random dot pattern of 20% density of bright dots. B- photograph of moving dots. The camouflaged letter, though visible to the eye, is not visible to the camera. C- photograph of camouflaged letter in B with surround dots removed. D- two brief snapshots of the letter taken at different instants during the presentation. F,G- photographs of a typical random dot pattern, respectively of 1% and 0.1% density of bright dots. H,I- photographs of an uncamouflaged letter of, respectively, static and moving dots, density being 1% in both cases.



FACULTY OF ARTS

4700 KEELE STREET • NORTH YORK • ONTARIO • CANADA • M3J 1P3

Reports on the work completed to date have been submitted for publication^(13,14).

(5) *A simple device for testing visual sensitivity to motion-defined objects*

From the viewpoint of aviation, the significance of the findings reported in Section 2-5 above is that they suggest that in nap of the earth helicopter flight, where some ground features are visible by motion alone while others are visible by contrast, a pilot's visual judgements might fail for motion-visible objects but not for contrast-visible objects even though the motion-visible objects are still clearly visible. From the viewpoint of medical research, the significance is the suggestion that spatial vision for motion-defined form is mediated by different neurons than spatial vision for contrast-defined form so that there may be forms of visual damage or visual abnormality that do not affect visual acuity or contrast sensitivity, but degrade spatial vision for motion-defined objects.

It is not practical to follow up these implications with the equipment used to obtain the data reported above, because that is "one-off" equipment of our own design and is, complex and nonportable. Therefore we have developed a simple device for testing visual sensitivity to motion-defined form with the intent of providing a means of applying this basic research in field studies of pilots and in hospital medical research.

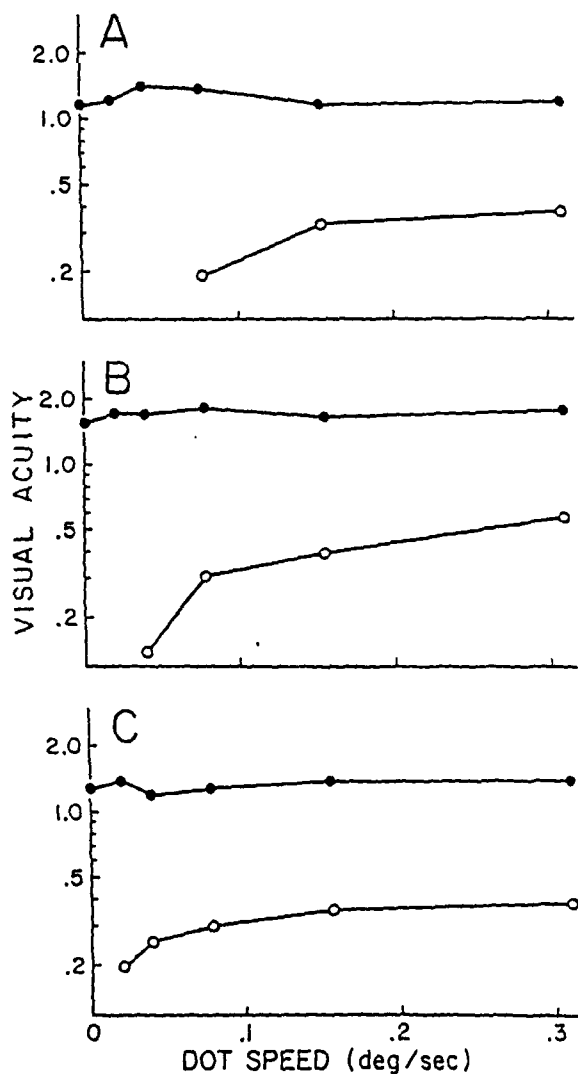


Figure 12 Ordinates plot visual acuity expressed as a Snellen fraction on a log scale. Abscissae plot dot speed on a linear scale. Open symbols indicate that letters were rendered visible by impressing equal and opposite speeds on the dots inside and outside the letter. Filled symbols indicate that letters were uncamouflaged as in Fig. 1C. Dot contrast was near 1.0 and dot density was 20%. Presentation duration was 4 sec viewing distance was 9 m. Panels A - C respectively show data for subjects 1, 3 and 5.

Figure 11 illustrates the principle. Figure 11A is a photograph of a random dot pattern generated on the screen of standard IBM PC. A letter (Z) at the centre of the screen is perfectly camouflaged. In Figure 11B, dots within the Z move rightwards and dots outside the Z move leftwards. The Z is visible to the normal eye, but is not visible to the camera. In Figure 11C, all dots outside the Z have been switched off so that the Z is defined by luminance contrast. The subject is required to read the letters presented. There are 10 letters for each of 9 letter sizes. Visual acuity for motion-defined letters can be measured at some given dot speed by plotting percent correct reading score versus letter size on probability paper, and reading off the letter size for a 75% correct score. Alternatively, speed threshold for a given letter size by plotting percent correct reading score versus dot speed on probability paper, and reading off the dot speed for a 75% correct score.

In order to thoroughly "de-bug" this test, an extensive parametric study on normally-sighted subjects was undertaken, and this has been published⁽¹⁵⁾. Figure 12 (open circles) shows that visual acuity for motion-defined letters falls off slowly as dot speed is reduced below 0.3 deg/sec until speed falls below a critical value below which acuity cannot be measured. On the other hand, visual acuity for a contrast-defined letter (Figure 11C) is essentially independent of dot speed. Open and closed circles in Figure 13 show, respectively, the effects of dot contrast on visual acuity for motion-defined and contrast-defined dotted letters. The effect of dot density is shown in Figure 14. Acuity for motion-defined letters (open circles) was comparatively unaffected by dot density from 50% to about 0.5%, (a 1000: 1 range) below which it abruptly collapsed. On the other hand, acuity

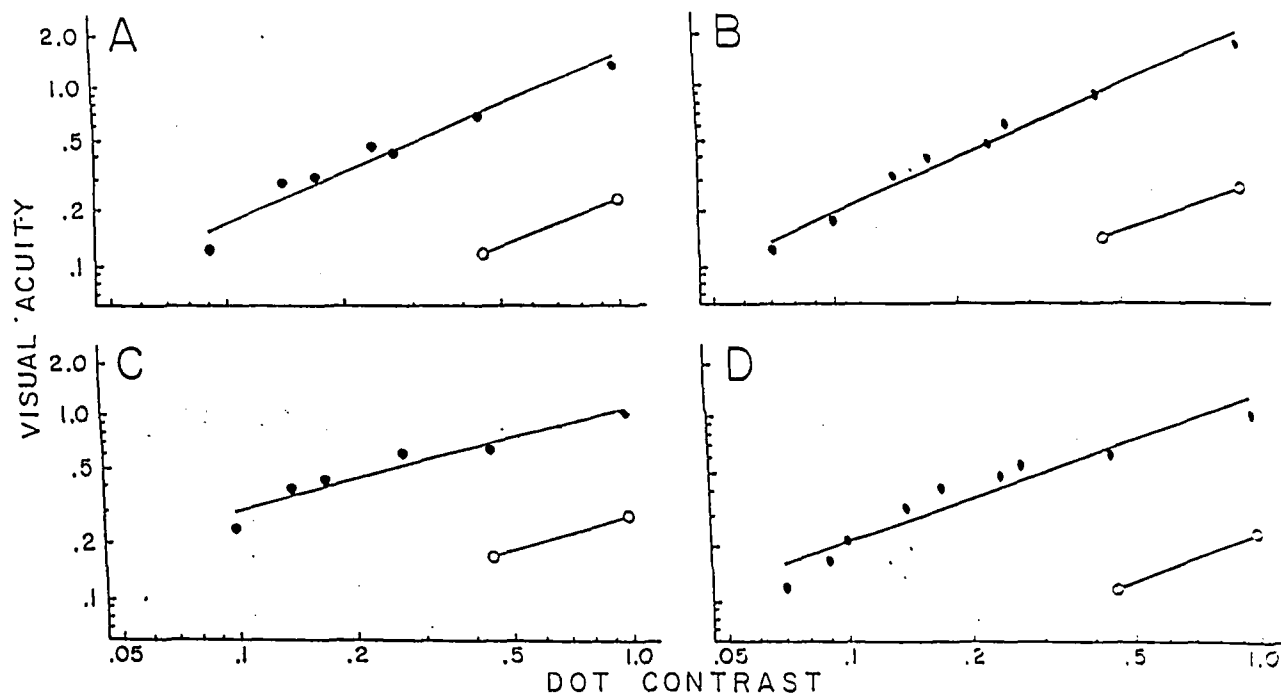


Figure 13. Ordinates plot visual acuity expressed as a Snellen fraction for dotted letters on a log scale. Abscissae plot dot contrasts on a log scale. Open symbols indicate that letters were rendered visible by impressing equal and opposite speeds of 0.47 deg/sec on dots inside and outside the letter. Filled symbols indicate that letters were uncamouflaged as in Fig. 1C with dot speed of 0.47 deg/sec. Dot density was 20%. Viewing distance was 6m. Presentation duration was 4 sec. Panels A-D respectively show data for subjects 1, 3, 2 and 6.

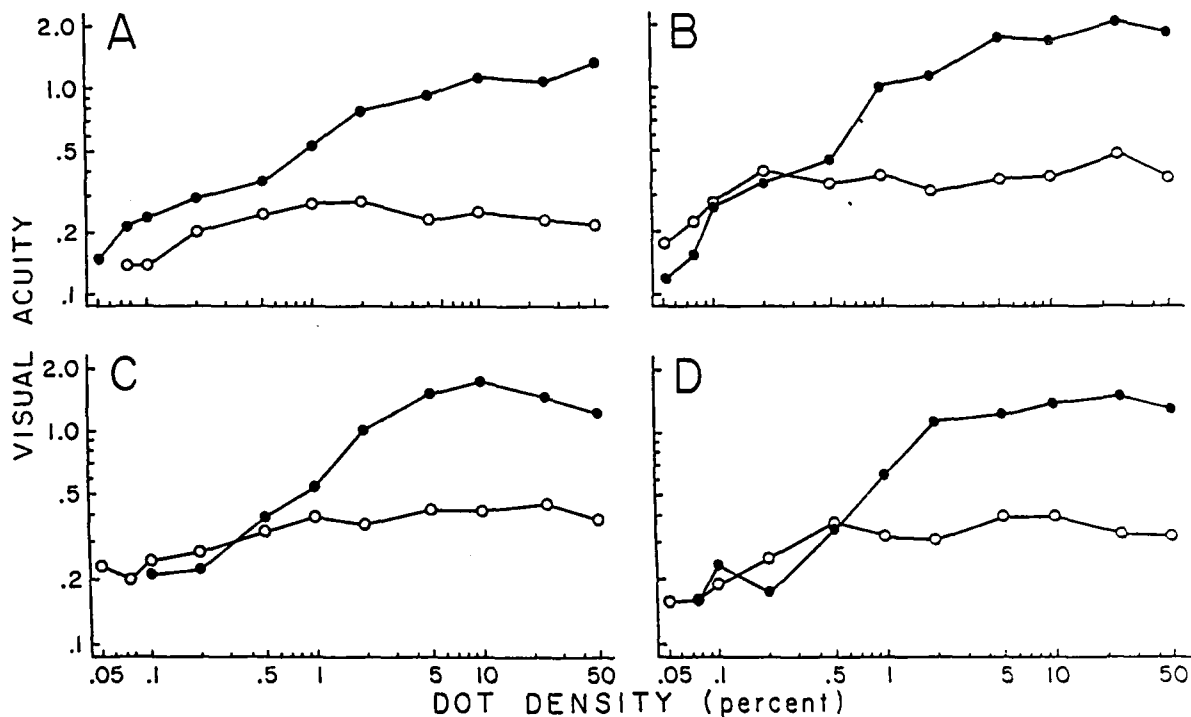
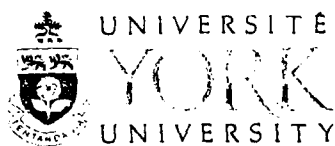


Figure 14 Ordinates plot visual acuity expressed as a Snellen fraction for dotted letters on a log scale. Abscissae plot the density of bright dots on a log scale. Open symbols, letters rendered visible by impressing equal and opposite speeds of 0.31 deg/sec on dots inside and outside the letters. Filled symbols, uncamouflaged letters as illustrated in Fig. 1C with dot speed of 0.31 deg/sec. Presentation duration was 4 sec. Dot contrast was 1.0. Viewing distance was 9m. Panels A-D respectively show data for subjects 1, 3, 5 and 4.



for contrast-defined letters (filled circles) progressively fell as dot density was reduced from 50%, and below about 0.5% approximated acuity for motion-defined letters.

(6) *Investigation of visual loss in patients with multiple sclerosis using the motion-defined letter test described in Section 6*

We have investigated 50 eyes of 25 patients with multiple sclerosis, and 50 eyes of 50 control subjects using the following tests: (A) Speed threshold for 75% correct reading score on large (6/60) motion-defined letters; (B) Contrast threshold for 75% correct reading score for 6/60 contrast-defined dotted letter; (C) Visual acuity for 75% correct reading score for motion-defined letters with a fixed, high, dot speed; (D) Visual acuity for solid, contrast-defined letters on the Regan low-contrast letter charts (96%, 11% and 4% letter contrasts); (E) Isolated-letter visual acuity using the same letters as on the Regan letter charts.

We found that speed threshold for motion-defined letters could detect visual abnormality that was not detected by any of the other tests used. Of the 50 eyes of patients, 34 (i.e. 68%) were abnormal at the 2.5 SD level, and of these 34 eyes, 5 were effectively motion blind in the sense that they could not read large letters even at our highest speed difference of 0.9 deg/sec. (Note that this is a new kind of motion blindness, quite different from the motion-in-depth blindness reported above). We conclude that our motion-defined letter test can detect pathology that is not picked up by testing contrast sensitivity or low-contrast acuity. We suggest that this new test can detect dysfunction in the human equivalent of a pathway in monkey brain that originates in large retinal ganglion cells, passes through the magnocellular layers of the lateral geniculate body, includes cortical area MT, and is involved in processing motion.

A manuscript is about to be submitted for publication⁽¹⁹⁾ and two abstracts are submitted (20,21).

(7) *Investigation of visual loss in patients with ocular hypertension and early glaucoma using the motion-defined letter test described in Section 6.*

This study is in progress. Twenty patients have been tested.

(8) *Investigation of visual loss in patients with Parkinson's disease.*

Toronto Western Hospital is one of the sites of the US/Canadian multi-centre trial of the new drug deprenyl and Professor A Lang, MD is Director of this site. This drug is thought to slow the progress of brain (nigral) damage caused by the disease, though it does not control the symptoms. (While conventional therapy controls the symptoms, the disease continues to progress). We and others have previously reported evidence suggesting that the motion pathway can be selectively affected in Parkinson's disease⁽¹⁶⁻¹⁸⁾. In a joint study with Dr. Lang we are asking whether our motion-defined letter test can provide an index of the functional integrity of dopaminergic neurons in the visual system, and if so whether this also provides an index of the patient's general clinical condition.

By comparing eye movement records with MR images, Dr. J.A. Sharp, Head of Neurology at the University of Toronto has discovered that eye movements in response to a moving target are defective in humans with focal brain lesions in an area of cortex suspected to be equivalent to MT and MST in macaque. It is known that damage to MT in macaque causes eye movement defects and also behavioural defects in motion processing. We are currently carrying out a joint study with Dr. Lang to compare pursuit eye movements with reading scores for motion-defined targets in patients with Parkinson's disease and patients with focal brain lesions.



2b. Status of the research effort: neuromagnetism and electrophysiology

(9) Theoretical and technical work on the two-input technique for characterizing nonlinear processing in sensory pathways

Neurons that respond asymmetrically – e.g. to leftwards versus rightwards motion, to increase versus decrease of spatial contrast, or to rise versus fall of auditory tone frequency – can be described as rectifiers. In addition to asymmetric response, many neurons perform functionally – important nonlinear processing such as ratio-ing,⁽²²⁻²⁴⁾ multiplication,⁽²⁵⁾ or logarithmic compression.

We have developed a theoretical basis and a practical technique for investigating nonlinear processing in sensory pathways. The basic procedure can be traced back at least to Bennet's 1933 paper⁽²⁶⁾ on radio communication. In general terms, Bennet's basic idea was to stimulate the nonlinearity being studied with two simultaneous inputs, one of temporal frequency F_1 Hz and the other of F_2 Hz. Any other frequency terms *must* be due to nonlinear processing.

Bennet⁽²⁶⁾ discussed the case of simple linear rectifier, and showed theoretically that the output included many terms of frequency $(nF_1 \pm mF_2)$, where n and m are integral or zero.

Bennet considered the case that the amplitude of the F_1 Hz input is held constant while the amplitude of the F_2 Hz input is progressively increased from zero, and developed a theoretical method for calculating how the amplitudes of the several discrete frequency terms vary with the F_2 Hz input amplitude.

Bennet's theoretical work was further developed by Rice but was not extended previously to rectifiers of any given characteristic nor to cascades of rectifiers.



We have made the following further steps. We have developed a theoretical treatment of the following cases: (a) single compressive rectifier, $y = x^{1/n}$; (b) single accelerating rectifier $y = x^n$; (c) cascaded sequence of rectifiers, e.g. multiple compressive third root rectifiers in series, and mixed cascaded rectifiers, e.g. compressive third root followed by accelerating square law; (d) two parallel rectifiers (compressive or accelerating) converging onto a third (compressive or accelerating); (e) a single rectifier whose characteristic matches the physiological contrast sensitivity characteristics, i.e. a threshold – initial acceleration – subsequent compression.⁽²⁷⁾

A sequence of cascaded rectifiers (c above) is intended to model a sequence of rectifier-like neurons as, for example, the photoreceptor–bipolar–ganglion cell–LGN cell–cortical cell sequence. Case (d) above is intended to model the dichoptic visual situation (i.e. signals leaving nonlinear processors in left and right eyes converging onto binocular cortical neurons) or the dichotic situation (i.e. signals leaving nonlinear processors in left and right ears converging onto binaurally-driven cells).

We went on to compute the amplitudes of several (up to 20) of the discrete nonlinear frequency components as a function of the amplitude of the F_2 Hz input.⁽²⁷⁾

In brief, this theoretical work suggests that *the resulting family of curves comprises a "fingerprint" of the type of nonlinearity. Because so many different frequency components are computed, just as with a human "fingerprint," there is high specificity, allowing different kinds of nonlinearity to be recognized.*

The following is an outline of this mathematical work. A full treatment of the work to date has been published in the *Journal of Theoretical Biology*.⁽²⁸⁾



A METHOD FOR DERIVING THE RESPONSE OF ASYMMETRIC NONLINEARITIES TO A SUM OF TWO SINEWAVES

We first consider the simple case of a half-wave linear rectifier fed with a single sinewave, and then with the sum of two sinewaves. After this introduction we go on to the accelerating and compressive rectifiers fed with the sum of two sinewaves, and finally discuss cascaded rectifiers and parallel-cascaded rectifiers of the same type and of mixed types.

[1] HALF-WAVE LINEAR RECTIFIER : RESPONSE TO A SINGLE SINUSOID.

Let the input to a half-wave rectifier ($y = cx$, $x \geq 0$; $y = 0$, $x < 0$) be $e(t) = A \cos(pt + \theta_p) = A \cos x$, where $p = 2\pi \times \text{frequency of input}$ and $\theta_p = \text{phase}$. Taking $A > 0$ and the constant of proportionality $c = 1$, the output is a function $f(x)$, where

$$f(x) = \begin{cases} A \cos x, & \cos x \geq 0 \\ 0, & \cos x < 0. \end{cases}$$

We can express $f(x)$ in terms of a Fourier series in x , where

$$f(x) = a_0/2 + \sum_{n=1}^{\infty} a_n \cos nx$$

and

$$\begin{aligned} a_n &= \frac{1}{\pi} \int_{-\pi/2}^{\pi/2} f(x) \cos nx \, dx, \quad f(x) = 0, \quad |x| > \pi/2, \quad n = 0, 1, 2, \dots \\ &= \frac{1}{\pi} \int_{-\pi/2}^{\pi/2} A \cos x \cos nx \, dx \\ &= \frac{A}{\pi} \int_0^{\pi/2} [\cos(n+1)x + \cos(n-1)x] \, dx, \quad n \neq 1 \\ &= \begin{cases} \frac{2A(-1)^{(n+1)/2}}{(n^2-1)\pi} & n \text{ even} \\ 0 & n \text{ odd}, \quad n \neq 1, \end{cases} \end{aligned}$$

$$\text{and} \quad a_1 = \frac{2}{\pi} \int_0^{\pi/2} \cos^2 x \, dx = \frac{1}{2}$$

$$\Rightarrow f(x) = \frac{A}{\pi} + \frac{A}{2} \cos x + \frac{2A}{3\pi} \cos 2x - \frac{2A}{15\pi} \cos 4x + \dots$$

[2] HALF-WAVE LINEAR RECTIFIER : RESPONSE TO THE SUM OF TWO SINUSOIDS



If the input voltage is given by

$$e(t) = P \cos(pt + \theta_p) + Q \cos(qt + \theta_q)$$

then we can rewrite this as

$$e(t) = P[\cos(pt + \theta_p) + k \cos(qt + \theta_q)]$$

where $k = Q/P$.

The case $k \leq 1$

Without loss of generality, we can take $P > 0$ and the constant of proportionality, c , to be 1. First let us consider $k \leq 1$, and set

$$f(x, y) = \begin{cases} P(\cos x + k \cos y), & (\cos x + k \cos y) \geq 0 \\ 0, & (\cos x + k \cos y) < 0 \end{cases}$$

where $x = (pt + \theta_p)$, and $y = (qt + \theta_q)$.

$f(x, y)$ is a surface in and above the (x, y) -plane, bounded by $(\cos x + k \cos y) = 0$ in the (x, y) -plane. Clearly adding 2π to x or y leaves $f(x, y)$ unaltered, so $f(x, y)$ is a periodic function in x and y . So if we know $f(x, y)$ in the rectangle $(-\pi, \pi) * (-\pi, \pi)$ we will know all its values.

Since $f(x, y)$ is bounded in the rectangle $(-\pi, \pi) * (-\pi, \pi)$ and its first derivatives are bounded, the double Fourier series in (x, y) of $f(x, y)$ is a valid expansion in this rectangle (Hobson, 1926). If the Fourier series of $f(x, y)$ is valid in the (x, y) plane, then it is valid on the line $py - qx = p\theta_q - q\theta_p$, found by eliminating t from $x = (pt + \theta_p)$, $y = (qt + \theta_q)$.

The boundaries of $f(x, y)$ are the curves given by $\cos x + k \cos y = 0$. In the shaded area, $\cos x + k \cos y \geq 0$, elsewhere $\cos x + k \cos y < 0$, giving $f(x, y) = 0$. Since $f(x, y)$ is an even function, its double Fourier expansion will be a cosine series given by

$$f(x, y) = \frac{1}{2} A_{00} + \sum_{m=1}^{\infty} \sum_{n=1}^{\infty} A_{\pm mn} \cos(mx \pm ny) + A_{10} \cos x + A_{01} \cos y$$

where

$$\begin{aligned} A_{\pm mn} &= \frac{1}{2\pi^2} \int_{-\pi}^{\pi} \int_{-\pi}^{\pi} f(x, y) \cos(mx \pm ny) dx dy \\ &= \frac{1}{2\pi^2} \int_{-\pi}^{\pi} \int_{-\pi}^{\pi} f(x, y) [\cos mx \cos ny \mp \sin mx \sin ny] dx dy. \end{aligned}$$



Since the region is symmetrical in both x and y , $A_{\pm mn}$ can be found by using one quarter of the plane. Hence

$$A_{\pm mn} = \frac{2P}{\pi^2} \int_0^\pi \cos ny \int_0^{\arccos(-k \cos y)} (\cos x + k \cos y) \cos mx \, dx \, dy$$

since $f(x, y) = 0$ when $x > \arccos(-k \cos y)$.

The calculation for $A_{\pm mn}$, when $m = 2$ and $n = 0$, is shown below.

$$\begin{aligned} A_{20} &= \frac{2P}{\pi^2} \int_0^\pi \int_0^{\arccos(-k \cos y)} (\cos x + k \cos y) \cos 2x \, dx \, dy \\ &= \frac{2P}{2\pi^2} \int_0^\pi (1 - k^2 \cos^2 y)^{3/2} dy \\ &= \frac{4P}{3\pi^2} \int_0^1 \frac{(1 - k^2 z^2)^{3/2}}{(1 - z^2)^{1/2}} dz \\ &= \frac{4P}{3\pi^2} \left\{ \int_0^1 \left(\frac{1 - k^2 z^2}{1 - z^2} \right)^{1/2} dz - \int_0^1 k^2 z^2 \left(\frac{1 - k^2 z^2}{1 - z^2} \right)^{1/2} dz \right\}. \end{aligned}$$

Using the identity

$$\left(\frac{(1 - k^2 z^2)}{(1 - z^2)} \right)^{1/2} = \left\{ \frac{1}{\{(1 - k^2 z^2)(1 - z^2)\}^{1/2}} - \frac{k^2 z^2}{\{(1 - k^2 z^2)(1 - z^2)\}^{1/2}} \right\}$$

and letting

$$Z_s = \int_0^1 \frac{z^s}{\{(1 - z^2)(1 - k^2 z^2)\}^{1/2}} dz$$

then $Z_0 = K$, the complete elliptic integral of the first kind, and Z_s can be expressed in terms of Z_{s-2} and Z_{s-4} by using the recurrence formula

$$Z_s = \frac{(s-2)(1+k^2)Z_{s-2} - (s-3)Z_{s-4}}{(s-1)k^2}$$

for $s \geq 4$, (Bennett, 1933). From

$$Z_2 = (K - E)/k^2,$$



where E is the complete elliptic integral of the second kind, we have that

$$\begin{aligned} A_{20} &= \frac{4P}{3\pi^2} [E - k^2 Z_2 + k^4 Z_4] \\ &= \frac{4P}{3\pi^2} [E - (K - E) + (2 + k^2)K/3 - 2(1 + k^2)E/3] \\ &= \frac{4P}{9\pi^2} [2(2 - k^2)E - (1 - k^2)K]. \end{aligned}$$

This gives the amplitude of the frequency $(mx \pm ny)/2\pi$ and the phase angle $(m\theta_p \pm n\theta_q)$. The values of the amplitudes for m and $n = 0, 1, 2, 3, 4$ are as follows :

$$\begin{aligned} A_{00} &= \frac{4P}{\pi^2} [2E - (1 - k^2)K] \\ A_{10} &= \frac{P}{2} \\ A_{01} &= \frac{kP}{2} \\ A_{20} &= \frac{4P}{9\pi^2} [2(2 - k^2)E - (1 - k^2)K] \\ A_{11} &= \frac{4P}{3\pi^2 k} [(1 + k^2)E - (1 - k^2)K] \\ A_{02} &= \frac{4P}{9\pi^2 k^2} [2(2k^2 - 1)E + (2 - 3k^2)(1 - k^2)K] \\ A_{40} &= \frac{4P}{225\pi^2} [(-38 + 88k^2 - 48k^4)E + (23 - 47k^2 + 24k^4)K] \\ A_{31} &= \frac{4P}{45\pi^2 k} [(8k^4 - 13k^2 + 3)E - (1 - k^2)(3 - 4k^2)K] \\ A_{22} &= \frac{4P}{15\pi^2 k^2} [(k^2 - 1)(k^2 - 2)K - 2(k^4 - k^2 + 1)E] \\ A_{13} &= \frac{4P}{45\pi^2 k^3} [(8 - 13k^2 + 3k^4)E - (8 - 17k^2 + 9k^4)K] \\ A_{04} &= \frac{4P}{225\pi^2 k^4} [(k^2 - 1)(-15k^4 + 64k^2 - 48)K - (38k^4 - 88k^2 + 48)E]. \end{aligned}$$

The third and higher odd order terms are zero, and

$$\begin{aligned} K &= \int_0^{\pi/2} (1 - k^2 \sin^2 \theta)^{-\frac{1}{2}} d\theta \\ &= \int_0^1 [(1 - z^2)(1 - k^2 z^2)]^{-\frac{1}{2}} dz \end{aligned}$$



and

$$\begin{aligned}
 E &= \int_0^{\pi/2} (1 - k^2 \sin^2 \theta)^{\frac{1}{2}} dz \\
 &= \int_0^1 (1 - k^2 z^2)^{\frac{1}{2}} (1 - z^2)^{-\frac{1}{2}} dz
 \end{aligned}$$

where $k \leq 1$.

The case $k > 1$.

We can rewrite $f(x, y)$ in the following way:

$$f(x, y) = \begin{cases} P(\cos y + l \cos x)/l, & \cos y + l \cos x \geq 0 \\ 0, & \cos y + l \cos x < 0 \end{cases}$$

where $l = 1/k < 1$ and consequently

$$f(x, y) = A'_{00}/2 + \sum_{r=1}^{\infty} \sum_{s=1}^{\infty} A'_{\pm rs} \cos(rx \pm sy) + A'_{10} \cos y + A'_{01} \cos x$$

where

$$A'_{\pm rs} = \frac{2P}{l\pi^2} \int_0^{\pi} \cos sx \int_0^{\arccos(-l \cos x)} (\cos y + l \cos x) \cos ry \, dy \, dx.$$

$A'_{\pm rs}$ is the coefficient of $\cos(rx \pm sy)$ which may be written as $\cos(sx \pm ry)$. So for a given m and n , say M and N , we will have to consider $A_{\pm MN}$, for $k \leq 1$ and $A'_{\pm NM}$ for $k > 1$. For example, let us consider the coefficient of $\cos 2x$.

$$\begin{aligned}
 A'_{\pm 02} &= \frac{2P}{l\pi^2} \int_0^{\pi} \cos 2x \int_0^{\arccos(-l \cos x)} (\cos y + l \cos x) \, dy \, dx \\
 &= \frac{4P}{9\pi^2 l^3} [2(2l^2 - 1)E + (2 - 3l^2)(1 - l^2)K] \\
 &= \frac{4Pk^3}{9\pi^2} [2(2/k^2 - 1)E(1/k) + (2 - 3/k^2)(1 - 1/k^2)K(1/k)] \\
 &= \frac{4P}{9\pi^2 k} [2k^2(2 - k^2)E(1/k) + (2k^2 - 3)(k^2 - 1)K(1/k)].
 \end{aligned}$$

Therefore the function of amplitude $g(k)_{\pm mn}$ is given by

$$g(k)_{\pm mn} = \begin{cases} A_{\pm mn}, & k \leq 1 \\ A'_{\pm nm}, & k > 1. \end{cases}$$



When $k > 1$, we have the following values for $A'_{\pm mn}$ when m and n are 0, 1, 2, 3, 4:

$$\begin{aligned}
 A'_{\pm 00} &= \frac{4P}{\pi^2 k} [2k^2 E - (k^2 - 1)K] \\
 A'_{\pm 10} &= \frac{kP}{2} \\
 A'_{\pm 01} &= \frac{P}{2} \\
 A'_{\pm 20} &= \frac{4P}{9\pi^2 k} [2(2k^2 - 1)E - (k^2 - 1)K] \\
 A'_{\pm 11} &= \frac{4P}{3\pi^2} [(k^2 + 1)E - (k^2 - 1)K] \\
 A'_{\pm 02} &= \frac{4P}{9\pi^2 k} [2k^2(2 - k^2)E + (2k^2 - 3)(k^2 - 1)K] \\
 A'_{\pm 40} &= \frac{4P}{225\pi^2 k^3} [(23k^4 - 47k^2 + 24)K + (-38k^4 + 88k^2 - 48)E] \\
 A'_{\pm 31} &= \frac{4P}{45\pi^2 k^2} [(8 - 13k^2 + 3k^4)E - (k^2 - 1)(3k^2 - 4)K] \\
 A'_{\pm 22} &= \frac{4P}{15\pi^2 k} [(1 - k^2)(1 - 2k^2)K - 2(1 - k^2 + k^4)E] \\
 A'_{\pm 13} &= \frac{4P}{45\pi^2} [(8k^4 - 13k^2 + 3)E - (8k^4 - 17k^2 + 9)K] \\
 A'_{\pm 04} &= \frac{4P}{225\pi^2 k} [(1 - k^2)(-15 + 64k^2 - 48k^4)K - k^2(38 - 88k^2 + 48k^4)E].
 \end{aligned}$$

The third and higher odd order terms are zero, and E and K are functions of $1/k < 1$. The elliptical integrals were calculated using well-known algorithms (King, 1924. Regan, 1985).

[3] HALF-WAVE SQUARE LAW RECTIFIER : RESPONSE TO THE SUM OF TWO SINUSOIDS.

If the rectifier is of the form $y = cx^2, x \geq 0$ and $y = 0, x < 0$ and if $k \leq 1$ then, as for the half-wave linear rectifier, we can consider the rectifier's output as the function $f(x, y)$ where

$$f(x, y) = \begin{cases} P^2(\cos x + k \cos y)^2, & \cos x + k \cos y \geq 0 \\ 0, & \cos x + k \cos y < 0 \end{cases}$$

where $x = (pt + \theta_p)$, and $y = (qt + \theta_q)$. Again $f(x, y)$ is bounded in the rectangle $(-\pi, \pi) * (-\pi, \pi)$ by $\cos x + k \cos y$ and its Fourier expansion will be a cosine series given



by

$$f(x, y) = \frac{1}{2}A_{00} + \sum_{m=1}^{\infty} \sum_{n=1}^{\infty} A_{\pm mn} \cos(mx \pm ny) + A_{10} \cos x + A_{01} \cos y$$

but now

$$A_{\pm mn} = \frac{2P^2}{\pi^2} \int_0^{\pi} \cos ny \int_0^{\arccos(-k \cos y)} (\cos x + k \cos y)^2 \cos mx \, dx \, dy$$

since $f(x, y) = 0$ when $x > \arccos(-k \cos y)$. When $k > 1$, we have

$$\begin{aligned} A'_{\pm rs} &= \frac{2P^2}{l^2 \pi^2} \int_0^{\pi} \cos sx \int_0^{\arccos(-l \cos x)} (\cos y + l \cos x)^2 \cos ry \, dy \, dx \\ &= \frac{2P^2 k^2}{\pi^2} \int_0^{\pi} \cos sx \int_0^{\arccos(-l \cos x)} (\cos y + l \cos x)^2 \cos ry \, dy \, dx \end{aligned}$$

where $l = 1/k$.

[4] HALF-WAVE SQUARE-ROOT RECTIFIER : RESPONSE TO THE SUM OF TWO SINUSOIDS.

Now the rectifier is of the form $y = c\sqrt{x}$, $x \geq 0$ and $y = 0$, $x < 0$ and for $k \leq 1$ we will have the function

$$f(x, y) = \begin{cases} P^{\frac{1}{2}} (\cos x + k \cos y)^{\frac{1}{2}}, & \cos x + k \cos y \geq 0 \\ 0, & \cos x + k \cos y < 0 \end{cases}$$

where $x = (pt + \theta_p)$, and $y = (qt + \theta_q)$. Thus

$$A_{\pm mn} = \frac{2P^{\frac{1}{2}}}{\pi^2} \int_0^{\pi} \cos ny \int_0^{\arccos(-k \cos y)} (\cos x + k \cos y)^{\frac{1}{2}} \cos mx \, dx \, dy$$

since $f(x, y) = 0$ when $x > \arccos(-k \cos y)$ and for $k > 1$, we have

$$\begin{aligned} A'_{\pm rs} &= \frac{2P^{\frac{1}{2}}}{l^{\frac{1}{2}} \pi^2} \int_0^{\pi} \cos sx \int_0^{\arccos(-l \cos x)} (\cos y + l \cos x)^{\frac{1}{2}} \cos ry \, dy \, dx \\ &= \frac{2P^{\frac{1}{2}} k^{\frac{1}{2}}}{\pi^2} \int_0^{\pi} \cos sx \int_0^{\arccos(-l \cos x)} (\cos y + l \cos x)^{\frac{1}{2}} \cos ry \, dy \, dx \end{aligned}$$

where $l = 1/k$. Similarly, we can find the response to any half-wave rectifier whose equation is $y = cx^n$, $x \geq 0$; $y = 0$, $x < 0$, where n is any real number.



[5] TWO CASCADED LINEAR HALF-WAVE RECTIFIERS, A.C. COUPLED.

If two rectifiers are D.C. coupled, the output will be the same as a single linear half-wave rectifier. Indeed, if two half-wave rectifiers are D.C. coupled and the first of the series is a linear rectifier, the final output will be the same as that of the second rectifier alone.

After the two sinusoids pass through the first rectifier, their function is given by

$$f(x, y) = \begin{cases} P(\cos x + k \cos y), & (\cos x + k \cos y) \geq 0 \\ 0, & (\cos x + k \cos y) < 0 \end{cases}$$

where $x = (pt + \theta_p)$, and $y = (qt + \theta_q)$. This has a D.C.-level given by $A_{00}/2$, the constant term in the double Fourier series expansion of $f(x, y)$. If our two successive rectifiers are linked by A.C. coupling, this D.C.-level must be removed and so the function entering the second rectifier is given by

$$F(x, y) = f(x, y) - A_{00}/2$$

where

$$A_{00} = \frac{2P}{\pi^2} \int_0^\pi \int_0^{\arccos(-k \cos y)} (\cos x + k \cos y) dx dy.$$

After passing through the second rectifier, the output is given by

$$\phi(x, y) = \begin{cases} F(x, y), & F(x, y) \geq 0 \\ 0, & F(x, y) < 0. \end{cases}$$

This can be represented by a double Fourier series where the coefficients $A_{\pm mn}$ are given by

$$A_{\pm mn} = \frac{2P}{\pi^2} \int_0^\pi \cos ny \int_0^\pi \phi(x, y) \cos mx dx dy.$$

[6] CASCADED COMPRESSIVE RECTIFIERS

Results have been obtained for two square root ($y = cx^{\frac{1}{2}}, x \geq 0; y = 0, x < 0$) rectifiers in series in particular, for any combination of two compressive rectifiers ($y = cx^N, x \geq 0; y = 0, x < 0$ and $\leq N \leq 1$) and for three square root rectifiers in series.

[7] TWO PARALLEL LINEAR RECTIFIERS WHOSE SUMMED OUTPUTS PASS THROUGH A THIRD LINEAR RECTIFIER: THE DICHOTIC OR DICHOTIC CASE



In this situation one only frequency ($F1$) passes through rectifier no. 1 and only one frequency ($F2$) passes through rectifier no.2 in parallel with the first rectifier. Then the output from both rectifiers combine to form the input of the third rectifier.

The output of the first rectifier is $f(x)$ where

$$f(x) = \begin{cases} P \cos x, & \cos x \geq 0 \\ 0, & \cos x < 0 \end{cases}$$

with a D.C.-level of P/π . The output of the second rectifier is $g(y)$ where

$$g(y) = \begin{cases} Pk \cos y, & \cos y \geq 0 \\ 0, & \cos y < 0 \end{cases}$$

whose D.C.-level is Pk/π . To adjust for the D.C.-level, the input to the third rectifier will be the function

$$h(x, y) = f(x) - P/\pi + g(y) - Pk/\pi.$$

The output from the third rectifier is given by

$$H(x, y) = \begin{cases} h(x, y), & h(x, y) \geq 0 \\ 0, & h(x, y) < 0. \end{cases}$$

Hence the coefficients of the double Fourier series can be found for

$$A_{\pm mn} = \frac{2P}{\pi^2} \int_0^\pi \cos ny \int_0^\pi H(x, y) \cos mx dx dy$$

Results have been obtained for the case that all three rectifiers have a linear characteristic and coupling is A.C. rather than D.C. Other cases such as mixed rectifiers (e.g. where nos.1 and 2 are cube root rectifiers and no.3 is a square law rectifier) are amenable to the same general mathematical treatment.

[8] HALF-WAVE RECTIFIER COMBINING ACCELERATING AND COMPRESSIVE SEGMENTS

For this rectifier, the curve equation is given by

$$y = \begin{cases} 0, & x < c \\ d(x - c)^4, & c \leq x < 5c \\ (x - c)^{1/16} - g, & 5c \leq x \end{cases}$$



where $d = 1/64(4c)^{\frac{63}{16}}$ and $g = \frac{63}{64}(4c)^{\frac{1}{16}}$ and c is chosen suitably. Consequently

$$f(x, y) = \begin{cases} 0, & \cos x + k \cos y < c \\ P^4 d (\cos x + k \cos y - \frac{c}{P})^4, & c \leq \cos x + k \cos y < 5c \\ P^{\frac{1}{16}} (\cos x + k \cos y - \frac{c}{P})^{\frac{1}{16}} - g, & 5c \leq \cos x + k \cos y \end{cases}$$

where $x = (pt + \theta_p)$, and $y = (qt + \theta_q)$. So

$$A_{\pm mn} = \frac{2}{\pi^2} \int_0^\pi \cos ny \int_0^\pi f(x, y) \cos mx \, dx \, dy$$

REFERENCES

- 1 Bennett, W.R. (1933) New Results in the Calculation of Modulation Products, Bell System Technical Journal, 228-243.
- 2 Hobson, E.W. (1926) *The Theory of Functions of a Real Variable and the Theory of Fourier's series*. Cambridge University Press, 710.
- 3 King, L.V. (1924) *On the direct Numerical Calculation of Elliptic Functions and Integrals*, Cambridge University Press.
- 4 Regan, M.P. (1985) Thesis, Dalhousie University.



(10) *Nondestructive zoom-FFT*

According to the Heisenberg-Gabor uncertainty principle the limiting frequency resolution of a spectrum, ΔF Hz, is given by

$$\Delta F = 1/\Delta T$$

where ΔT is the recording duration. Thus, for example, a recording of duration 500 sec could, in principle, be analyzed at a resolution of 0.002 Hz so that, if the bandwidth were DC–100 Hz, the spectrum would contain $100 \times 500 = 50,000$ lines. In practice, however, the FFT usually provides many fewer lines, typically several hundred over a DC–100 Hz bandwidth. We have developed a nondestructive form of zoom FFT that allows high zoom ratios (typically 32–64) over a wide bandwidth so that we routinely obtain 25,000 or 50,000 lines over DC–100 Hz.

The method is to digitize a time series of duration ΔT by means of a Bruel and Kjaer spectral analyzer. The digitized time series is recorded on floppy disk in an Hewlett-Packard model 9000 computer that controls the analyzer. If, for example, the bandwidth is DC–100 Hz, the sampling rate will be 250 Hz. We routinely digitize a 320-sec duration of the time series. Next, the digitized data are replayed at much increased rate (25 kHz rather than 250 Hz), filtered and, for example, the DC–3.0 Hz section submitted to FFT, giving 800 lines within DC–3.0 Hz. This destroys the time series in the analyzer. Now the time series is replayed again at 25 kHz, heterodyned to shift the 3.0–6.0 Hz segment to DC–3.0 Hz, filtered, resampled, submitted to FFT and shifted back to 3.0–6.0 Hz. This gives us 800 lines within 3.0–6.0 Hz. The process is repeated to give 800 lines in each 3.0 Hz segment between DC and 100 Hz.

The value of this method in electrophysiology is not self-evident. The value is based on our fortunate discovery, illustrated in Figure 15, that the discrete frequency components of the



steady-state evoked potential are of ultra-narrow bandwidth, and can be less than 0.002 Hz. Consequently, the noise is spread through 50,000 bins while signal components are concentrated into one or two bins. This gives (a) high signal-to-noise ratios, and (b) excellent separation of signal components. The procedure has been published in a book, sponsored in part by AFOSR⁽²⁹⁾ and is also in press in a journal article.⁽³⁰⁾

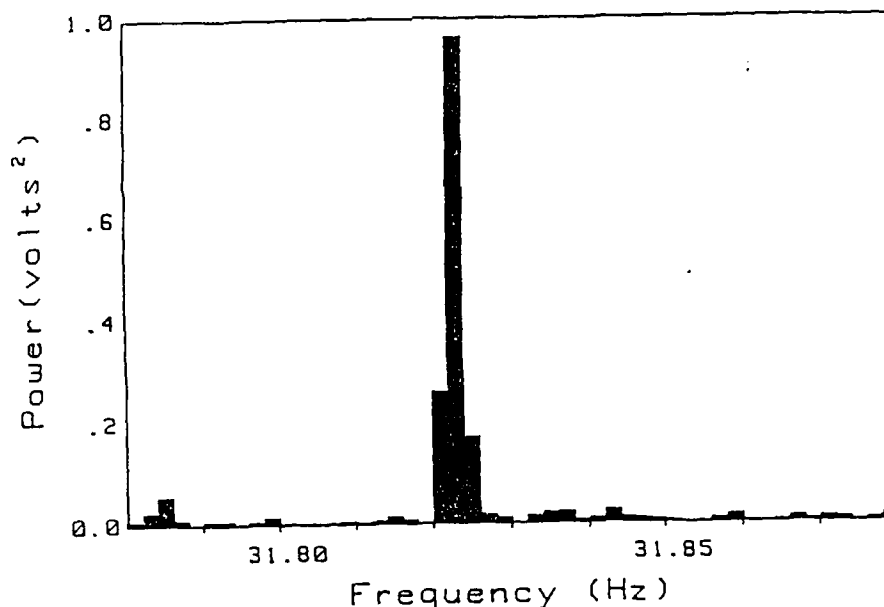


Figure 15. Two-Thousandth of a Hertz Bandwidth At a frequency of 0.0019 Hz approximately two thirds of the EP signal power is contained within a single bin. Therefore the EP signal's bandwidth is no more than 0.0019 Hz. Note that even if the EP signal's bandwidth were considerably less than 0.0019 Hz, more than one bin of the analyzer would contain power when the analyzer's resolution is set at 0.0019 Hz, because the sensitivity of adjacent bins overlaps. The stimulus was a vertical sine wave grating that was counterphase-modulated at nominally $F = 8$ Hz. The $4F$ component is shown. Zoom FFT was applied to the entire length of EEG samples of 520-sec duration. To allow some frequency-domain averaging (with overlap), recording duration was 640 sec.



(11) *Use of the two-sinewave method to measure orientation tuning in human cortical neurons*

A vertical sinewave grating of spatial frequency 5 c/deg was generated on a Joyce CRT and counterphase-modulated at frequency F1 (nominally 8 Hz). A second grating of spatial frequency 5.5 c/deg and variable orientation was generated on a second Joyce CRT and counterphase-modulated at frequency F2 (nominally 7 Hz). The two gratings were optically superimposed. Field size was 10 deg, contrast was 40% for each grating and mean luminance was 250 cd/m². Calibration with a linear photocell showed that each CRT was quite linear: second harmonic distortion was below 0.1% of the fundamental component's power. Cross-modulation terms were essentially zero because different CRTs driven by different electronics generated the F1 Hz and F2 Hz gratings. Photocell calibration showed cross-modulation components to be less than 0.01% of the fundamental components' power.

Human steady-state evoked potentials were recorded between electrodes placed on the inion and midway between the inion and the vertex along the midline. Responses were analyzed in the frequency domain by a Bruel and Kjaer analyzer (model 2032) modified to carry out zoom-FFT nondestructively at high zoom factors over a wide bandwidth.⁽²⁹⁾ Resolution was 0.0078 Hz over a DC–100 Hz bandwidth for a 320-sec recording period, i.e. 12,800 frequency bins were available with frequency-domain averaging also.

The dashed line in Figure 16 plots the amplitude of a (2F1 + 2F2) cross-modulation response term as a function of the orientation difference between the gratings. This cross-modulation term necessarily indicates a nonlinear interaction between visual responses to the fixed vertical grating and the variable-orientation grating, and has previously been shown to be substantially independent of spatial phase.^(31,32) Figure 16 shows that the nonlinear interaction was large when

the gratings were parallel and fell to a minimum when their orientations differed by about 30 deg. The half-height full bandwidth of the curve is about 12 deg. The frequency-doubled $2F_1$ Hz response produced by the fixed vertical grating was suppressed when the two gratings were parallel, but the second grating had comparatively little effect when grating orientations differed by about 30 deg. Similar results were obtained for a second and third subject.

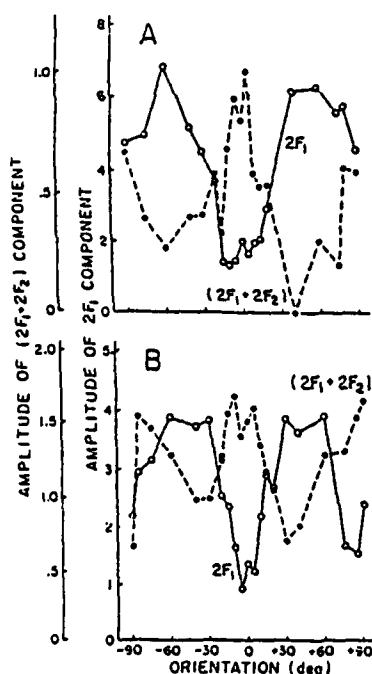


Figure 16. Nonlinear interactions between responses to two gratings as a function of orientation difference. A vertical grating was counterphase-modulated at F_1 Hz and a superimposed variable-orientation grating was modulated at F_2 Hz. Solid symbols plot the amplitude of the nonlinear cross-modulation $(2F_1 + 2F_2)$ Hz term in the evoked potential versus the variable grating's orientation. Open symbols plot the frequency-doubled $2F_1$ Hz term. Results are shown for two subjects.



The observations reported above can be understood if the $(2F1 + 2F2)$ term is generated by cortical neurons tuned to a narrow range of orientations (such as those described by De Valois *et al.*⁽³³⁾ When the grating orientations differ by more than about 30 deg, most of these neurons cannot encompass both gratings within their orientation bandwidths, and will therefore fail to generate cross-modulation terms.

However, when we placed the two gratings at right angles (the fixed grating remaining vertical), the nonlinear cross-modulation term rose to a second maximum. For subject B this $(2F1 + 2F2)$ term was as large for near-orthogonal gratings as for parallel gratings, and only a little less for subject A. The interaction term was largest at exactly 90 deg orientation difference for subject A but, curiously, peaked sharply just 5 deg from 90 deg for subject B.

This finding that there is a strong nonlinear interaction between responses to vertical and near-horizontal gratings can be understood if we assume that cortical neurons tuned to a narrow range of orientations around the vertical interact nonlinearly with cortical neurons tuned to a narrow range of orientations around the horizontal. It may be relevant that cortical neurons tuned to different orientations can inhibit each other when excited simultaneously.^(34,35)

If our findings can be generalized to other kinds of two-dimensional pattern, this would imply that human VEPs to patterns modulated in two dimensions cannot entirely be explained in terms of VEPs to gratings. In particular, the findings reported here could not result from the stimulation of independent, linear, orientation-selective mechanisms.

(12) *Nonlinear interactions between visual responses to two gratings of different spatial frequencies*

We have measured interactions between responses to two parallel or orthogonal gratings of different spatial frequencies. Subjects viewed a fixed 1.0 c/deg vertical grating counterphase modulated at $F_1 = 8$ Hz superimposed on a grating of variable spatial frequency and orientation, modulated at $F_2 = 7$ Hz. We analysed brain responses using high-resolution zoom-FFT, at a frequency resolution of 0.008 Hz (12,500 lines DC-100 Hz). Nonlinear processing produces multiple discrete components of frequency ($nF_1 \pm mF_2$) where n, m are zero or integral. We recorded up to 20 such discrete components, each with a bandwidth as narrow as 0.002 Hz. With parallel vertical gratings, the $2F_1$ Hz response of the 1 c/deg grating was suppressed nonlinearly by a second grating of higher spatial frequency over a broad 1.5-13 c/deg range, but the suppression did not occur in the opposite direction from low to high spatial frequency. Interactions between orthogonal gratings were qualitatively different. The $2F_1$ Hz response of the vertical 1.0 c/deg grating and the $2F_2$ Hz response of a 1.5-4 c/deg horizontal grating were both attenuated, suppression being exerted both ways along the spatial frequency axis. And with a horizontal grating of 4-13 c/deg there was comparatively little suppression of $2F_1$ and $2F_2$ components.

This work was reported at ARVO⁽³⁶⁾ and a manuscript is in preparation.

(13) *Animal experiments: Nonlinear analysis of single-cell firing and local slow potentials in anesthetized cat.*

This is a joint study (M.P. Regan, K. Grasse and D. Regan) and is in progress. The aim is to apply the mathematical and zoom-FFT approach described in Section 2b (4) above to single-cell recording of cortical cells so as (A) to develop a means of modelling the multi-neuron sequence of processing between retina and cortex; (B) to develop a new means of studying nonlinearities of



single cells, and (C) to find whether the very considerable stability of neural signals implied by the narrow bandwidth of the human evoked potential signals (Figure 13) is evident at single cell level or whether it is a multi-neuron property.

In order to carry out this study I have developed an electronic device for converting the instantaneous firing frequency of a single neuron into an analog signal that can be subjected to nondestructive zoom-FFT analysis as described in Section 2b (4) above. Visual stimulation equipment has been installed in Dr. Grasse's animal laboratory and connected to the zoom-FFT analyser in my laboratory. We have recorded from three cats and shown that nonlinear interactions between responses to two gratings can be analysed in cortical slow waves. We have recorded single-cell firing in striate cortex, and established the appropriate stimulus conditions.

(14) *Installation of the BTi 7-channel Neuromagnetometer and magnetically shielded room*

Installation of the magnetically shielded room started on September 12, 1988 in a room set aside for the purpose in the Farquarson Building at York University. Installation was completed on schedule. Installation of the neuromagnetometer was started on October 5, 1988. The system dewar was cooled to liquid helium temperature during the week of November 7, and has been maintained at liquid helium temperatures since then. Several of the students, technicians and faculty at York have been trained to transfer liquid helium from a 100-litre reservoir to the system dewar. This must be done three times a week. The total expenditure of liquid helium is stabilizing at about 100 litres per two weeks. BTi representatives continued to install and check out the magnetometer up to November 11, and throughout the week of November 14–18, five of us were instructed by BTi representatives on the use of the computer system and recording procedures.



In early 1989 BTi installed a sensory position indicator (SPI) on the magnetometer. Subsequent to installation one of the recording channels developed an intermittent fault. After considerable investigation this was shown in November 1989 to be caused by hardware damage, probably caused during SPI installation.

(15) *Analysis of human magnetic brain responses by nondestructive zoom-FFT*

Figure 17 shows evoked magnetic brain responses analysed by zoom-FFT at a resolution of 0.008 Hz. In Figure 17A the subject's contralateral ear was stimulated with a 1000 Hz tone that was amplitude modulated at $F_1 = 20.351$ Hz. The spike was at $2F_1 = 40.703$ Hz. In panel B the 1000 Hz tone was modulated at $F_2 = 20.742$ Hz. This spike was at $2F_2 = 41.484$ Hz. In panel C, the ear was stimulated with both AM tones simultaneously. The spikes in A and B were suppressed, and a new spike at $(F_1 + F_2) = 41.093$ Hz emerged.

The very narrow bandwidth of the spikes indicates that the steady-state magnetic response is very stable in amplitude and phase. This was observed at all recording sites (only one is shown). The nonlinear phenomenon shown in Figure 17 was replicated when we applied the stimulus to a hardware model of the ear's hair cell transducer function.

One of use (M.P. Regan) is developing a mathematical approach to modelling responses such as those shown in Figure 17 so as to allow neuromagnetic data to be used to test multi-neuron models of the auditory pathway.

This work is in press^(37,18) and a review article has been published⁽³⁹⁾.

(16) *Joint work with Professor L. Kaufman*

A joint experiment with Profesor L. Kaufman on the effects of attention on visual responses has been planned, and we have constructed the required apparatus.

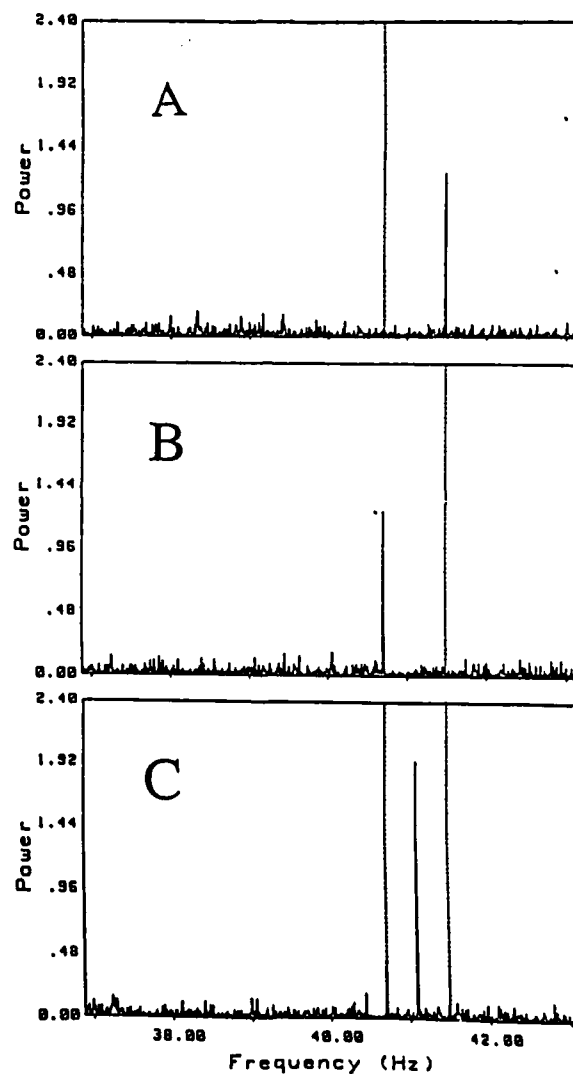


Figure 17. A small section of the MEG spectrum recorded during auditory stimulation. Analysis was by Zoom-FFT at a resolution of 0.008Hz.



- (17) *Book: "Human Brain Electrophysiology: Evoked potentials and evoked magnetic fields in science and medicine" by D. Regan*

Published by Elsevier 1989. This is a single-author book whose writing was sponsored in part by AFOSR. 820 pp, 372 figures.

This book attempts to link (1) our knowledge of evoked electrical and magnetic responses of the human brain to (2) sensory perception and cognition and (3) the properties of single neurons in primate brain. It covers vision, hearing, somatosensation and cognition. There are three parts: technical and mathematical aspects of recording techniques, basic research, and clinical applications. To date three journals have reviewed the book, and these reviews are quite favourable. Copies are enclosed.

- (18) *Editor of two books: "Binocular Vision" and "Spatial Form Vision"*

Macmillan is producing a series of about 14 volumes under the general title "Vision and Visual Abnormalities." I was invited to edit two of these books. My aim was to choose authors who had at least played an important innovative role in the development of their topic over the last 10-20 years and, preferentially, initiated major advances in their topic. In this way I hoped that authors would produce unique insights into how modern understanding of the topics really did emerge so as to provide students with a first-hand understanding of creative science that is often lacking in second-hand accounts. The authors were asked to review their topics at the level of a senior researcher while making the chapter accessible to graduate students. The teaching aspect was emphasized.



I was fortunate that almost all of my first choice authors agreed to contribute, and only very few topics had to be omitted. Both books are in press for a 1990 publication date. I am confident that the books will be of considerable use to the psychophysics, human factors and single-unit research communities.

MACMILLAN VOL. 10 "BINOCULAR VISION"

- H. Collewyn, R.M. Steinman, C.J. Erkelens and D. Regan, "Binocular fusion, stereopsis and Stereoacuity with a Moving Head".
J.M. Foley, "Binocular spare perception"
R. Fox, "Binocular rivalry"
R. Held, "Development of binocularity and stereopsis"
A.E. Kertesz, "Cyclofusion"
H. Ono, "Binocular visual directions of an object when seen as single or double"
G. Poggio, "Physiological basis of stereoscopic vision"
D. Regan, "Depth from motion and motion in depth"
C. Schor, "Binocular sensory disorders"
C.W. Tyler, "The horopter"
C.W. Tyler, "Cyclopean vision"



MACMILLAN 11 "SPATIAL VISION"

- J.R. Bergen, "Theories of visual texture perception"
I. Bodis-Wollner and D. Regan, "Spatio-temporal vision in Parkinson's disease and MPTP treated monkeys: the role of dopamine"
D. Levy, "Spatial vision in amblyopia"
G. Mohn and J. Van Hof-van Duin, "Development of spatial vision"
M. Morgan, "Hyperacuity"
G.T. Plant, "Temporal properties of normal and abnormal spatial vision"
D. Regan, "A brief review of some of the stimuli and analysis methods used in spatiotemporal vision research"
D. Regan, "Spatial vision for objects defined by colour contrast, binocular disparity and motion parallax"
D. Regan, "Spatial vision in multiple sclerosis"
K. Ruddock, "Spatial vision after cortical lesions"
R. Shapley, "Contrast sensitivity: neural mechanisms"
H.R. Wilson, "Psychophysical models of spatial vision and hyperacuity"



References

- (1) Regan D (1982) Visual information channeling in normal and disordered vision. *Psychol Rev* 89, 407-44.
- (2) Regan D & Beverley KI (1983) Spatial frequency discrimination and detection: comparison of postadaptation thresholds. *J Opt Soc Am* 73, 1684-90.
- (3) Regan D & Beverley KI (1985) Postadaptation orientation discrimination. *J Opt Soc Am A* 2, 147-55.
- (4) Wilson HR & Gelb DJ (1984) Modified line element theory. *J Opt Soc Am A* 1, 124-131.
- (5) Wilson HR & Regan D (1984) Spatial frequency adaptation and grating discrimination predictions of a line element model. *J Opt Soc Am A* 1, 1091-6.
- (6) Richards W & Regan D (1973) A stereo field map with implications for disparity processing. *Invest Ophthalmol* 12, 904-909.
- (7) Regan D, Erkelens CJ & Collewijn H (1986) Visual field defects for vergence eye movements and for stereomotion perception. *Invest Ophthalmol Vis Sci* 27, 806-819.
- (8) Hong X & Regan D (1989) Visual field defects for unidirectional and oscillatory motion in depth. *Vision Res* 29, 809-819.
- (9) Regan D (1989) Form from motion 3parallax and form from luminance contrast: vernier discrimination. *Spatial Vision* 1, 305-18.
- (10) Regan D (1989) Orientation discrimination for objects defined by relative motion and objects defined by luminance contrast. *Vision Res* 29, 1389-1400.
- (11) Beverley KI & Regan D (1980) Visual sensitivity to the shape and size of a moving object: implications for models of object perception. *Perception*, 9, 151-160.
- (12) Regan D. (1989) Shape discrimination for motion-defined objects. *Perception*, submitted.
- (13) Regan D & Hamstra S (1989) Shape discrimination for objects defined by relative motion: effects of presentation duration. *Vision Res*, submitted.
- (14) Regan D & Hamstra S (1989) Shape and orientation discrimination for motion-defined and contrast-defined objects: temporal integration. Submitted for ARVO 1990.
- (15) Regan D & Hong XH (1990) Visual acuity for optotypes made visible by relative motion. *Invest Ophthalmol Vis Sci*, January.
- (16) Regan D & Maxner C (1987) Orientation-selective visual loss in patients with Parkinson's disease. *Brain* 110, 239-271.
- (17) Bodis-Wollner I & Regan D (1989) Spatio-temporal contrast vision in Parkinson's disease and MPTP treated monkeys: the role of dopamine. In D. Regan (Ed) *Spatial Vision*. London: Macmillan, in press.



- (18) Bodis Wollner I, Marx MS, Mitra S, Bobak P, Mylin L & Yahr M (1987) Visual dysfunction in Parkinson's disease. *Brain*, 110, 1675-1698.
- (19) Regan D, Kothe A & Sharpe JA (1990) Recognition of motion-defined shapes in patients with multiple sclerosis. *Brain*, in preparation.
- (20) Kothe A, Regan D & Sharpe JA. Motion blindness and motion insensitivity in patients with multiple sclerosis. Submitted for ARVO 1990.
- (21) Kothe A, Regan D & Sharpe JA. Motion blindness and motion insensitivity in patients with multiple sclerosis. Submitted for Assoc. Can. Neurologists, 1990;
- (22) Regan D & Beverley KI (1983) Spatial frequency discrimination and detection: comparison of postadaptation thresholds. *J Opt Soc Am* 73, 1684-90.
- (23) Regan D & Beverley KI (1985) Postadaptation orientation discrimination. *J Opt Soc Am A2*, 147-55.
- (24) Beverley KI & Regan D (1973) Evidence for the existence of neural mechanisms selectively sensitive to the direction of movement in space. *J Physiol* 235, 17-29.
- (25) Morgan MJ & Regan D (1987) Opponent model for line interval discrimination: interval and vernier performance compared. *Vision Res* 27, 107-18.
- (26) Bennet WR (1933) *Bell Syst Tech J* 228-43.
- (27) Regan D (1989) *Human brain electrophysiology: Evoked potentials and evoked magnetic fields in science and medicine*. New York: Elsevier.
- (28) Regan MP & Regan D (1988) A frequency domain technique for characterizing nonlinearities in biological systems. *J Theoret Biol* 133, 293-317.
- (29) Regan D (1989) *Human brain electrophysiology: Evoked potentials and evoked magnetic fields in science and medicine*. New York: Elsevier.
- (30) Regan MP & Regan D (1988) Objective investigation of visual function using a non-destructive zoom-FFT technique for evoked potential analysis. *Can J Neurol Sci*, 16, 168-179.
- (31) Regan D & Regan MP (1987) Spatial frequency tuning, orientational tuning and spatial discrimination investigated by nonlinear analysis of pattern evoked potentials. In C Barber & T. Blum (Eds.) *Evoked Potentials III*, Butterworths, Stoneham M.A.
- (32) Regan D & Regan MP (1988) Objective evidence for phase-independent spatial frequency analysis in the human visual pathway. *Vision Res* 28, 187-91.
- (33) De Valois RL, Yund EW & Hepler N (1982) The orientation and direction selectivity of cells in macaque visual cortex. *Vision Res* 22, 531-544.
- (34) Bishop PO, Coombs JS & Henry GH (1973) Receptive fields of simple cells in the cat striate cortex. *J Physiol* 231, 31-60.



FACULTY OF ARTS

4700 KEELE STREET • NORTH YORK • ONTARIO • CANADA • M3J 1P3

- (35) Sillito AM, Kemp A, Milson JA & Berardi N (1980) A re-evaluation of the mechanisms underlying simple cell orientation selectivity. *Brain Res* 194, 517-20.
- (36) Regan MP & Regan D (1989) Nonlinear interactions between responses to difference spatial frequencies. ARVO abstracts. Invest Ophthal Suppl.
- (37) Regan D & Regan MP (1989) Ultra-high resolution analysis of auditory and visual brain responses using zoom-FFT. Proc. 7th Internat Conf Biomagnetism, in press.
- (38) Regan MP & Regan D (1989) A frequency domain technique for using evoked magnetic fields to test multi-stage models of sensory processing. Proc. 7th Internat Conf Biomagnetism, in press.
- (39) Regan D (1989) Magnetic fields generated by the human brain. *Can. Res* 22, 11-15.



PUBLICATIONS

Books:

- 1.Regan D (1972) Evoked potentials in psychology, sensory physiology and clinical medicine. London: Chapman & Hall; New York: Wiley, 328 pp, rpt 1975.
- 2.Regan D (1989) Human brain electrophysiology: Evoked potentials and evoked magnetic fields in science and medicine. New York: Elsevier, 672 pp.
- 3.Regan D, Shapley RM & Spekreijse H (Eds) (1985) Systems approach in vision. New York: Pergamon, 219 pp.
- 4.Regan D (Ed) (1989) Spatial Vision (Vol 10 in "Vision and visual dysfunction" series). London: Macmillan, in press.
- 5.Regan D (Ed) (1989) Binocular Vision (Vol 11 in "Vision and visual dysfunction" series). London: Macmillan, in press

PAPERS

- 1.Regan D (1966) Some characteristics of average steady-state and transient responses evoked by modulated light. *Electroenceph clin Neurophysiol* 20, 238-48.
- 2.Regan D (1966) An apparatus for the correlation of evoked potentials and repetitive stimuli. *Med Biol Engng* 4, 168-77.
- 3.Regan D (1966) An effect of stimulus colour on average steady-state potentials evoked in man. *Nature* 210, 1056-7.
- 4.Regan D (1968) A high frequency mechanism which underlies visual evoked potentials. *Electroenceph clin Neurophysiol* 25, 231-7.
- 5.Regan D (1968) Chromatic adaptation and steady-state evoked potentials. *Vision Res* 8, 149-58.
- 6.Regan D (1968) Evoked potentials and sensation. *Percept Psychophys* 4, 347-50.
- 7.Regan D (1969) Evoked potentials and colour vision. 7th ISCERG Symp, Istanbul. Univ of Istanbul, 37-50.
- 8.Regan D (1969) Chapters 3 & 4 in DM MacKay (Ed), Evoked potentials as indicators of sensory information processing. *Neurosci Res Bull* 7, N° 3.
- 9.Regan D & Heron JR (1969) Clinical investigation of lesions of the visual pathway: a new objective technique. *J Neurol Neurosurg Psychiat* 32, 479-83.
- 10.Tweel LH van der, Regan D & Spekreijse H (1969) Some aspects of potentials evoked by changes in spatial brightness contrast. 7th ISCERG Symp, Istanbul. Univ of Istanbul, 1-11.
- 11.Regan D (1970) Evoked potentials and psychophysical correlates of changes in stimulus colour and intensity. *Vision Res* 10, 163-78.
- 12.Regan D (1970) Objective method of measuring the relative spectral luminosity curve in man. *J Opt Soc Am* 60, 856-9.



- 13.Regan D & Heron JE (1970) Simultaneous recording of visual evoked potentials from the left and right hemispheres in migraine. In AL Cochrane (Ed), Background to migraine. London: Heinemann, 66-77.
- 14.Regan D & Cartwright RF (1970) A method of measuring the potentials evoked by simultaneous stimulation of different retinal regions. *Electroenceph clin Neurophysiol* 28, 314-9.
- 15.Regan D & Spekreijse H (1970) Electrophysiological correlate of binocular depth perception in man. *Nature* 255, 92-4.
- 16.Regan D & Sperling HG (1971) A method of evoking contour-specific scalp potentials by chromatic checkerboard patterns. *Vision Res* 11, 173-6.
- 17.Regan D & Tyler CW (1971) Wavelength-modulated light generator. *Vision Res* 11, 43-56.
- 18.Regan D & Tyler CW (1971) Some dynamic features of colour vision. *Vision Res* 11, 1307-24.
- 19.Regan D & Tyler CW (1971) Temporal summation and its limit for wavelength changes: an analog of Bloch's law for color vision. *J Opt Soc Am* 61, 1414-21.
- 20.Regan D & Richards W (1971) Independence of evoked potentials and apparent size. *Vision Res* 11, 679-84.
- 21.Regan D (1972) Evoked potentials to changes in the chromatic contrast and luminance contrast of checkerboard stimulus patterns. In GB Arden (Ed), *The visual system*. New York: Plenum, 171-87.
- 22.Regan D (1972) Evoked potentials to changes in chromatic contrast. *Proc GAIN symp on EPs to spatial contrast*. Trace 6, 20-8.
- 23.Regan D (1972) Cortical evoked potentials. *Adv Behav Biol* 5, 177-92.
- 24.Spekreijse H, van der Tweel LH & Regan D (1972) Interocular sustained suppression: correlations with evoked potential amplitude and distribution. *Vision Res* 12, 521-6.
- 25.Milner BA, Regan D & Heron JR (1972) Theoretical models of the generation of steady-state evoked potentials, their relation to neuroanatomy and their relevance to certain clinical problems. *Adv Med Biol* 24, 157-69.
- 26.Regan D (1973) Parallel and sequential processing of visual information in man: investigation by evoked potential recording. In *Photophysiology*, Vol 8. New York: Academic, 185-208.
- 27.Regan D (1973) An evoked potential correlate of colour: evoked potential findings and single-cell speculations. *Vision Res* 13, 1933-41.
- 28.Regan D (1973) Evoked potentials specific to spatial patterns of luminance and colour. *Vision Res* 13, 2381-2402.
- 29.Regan D (1973) Rapid objective refraction using evoked brain potentials. *Invest Ophthalmol* 12, 669-79.
- 30.Regan D & Richards W (1973) Brightness contrast and evoked potentials. *J Opt Soc Am* 63, 606-11.
- 31.Regan D & Beverley KI (1973) Disparity detectors in human depth perception: evidence for directional selectivity. *Science* 18, 877-9.
- 32.Regan D & Beverley KI (1973) Some dynamic features of depth perception. *Vision Res* 13, 2369-79.
- 33.Regan D & Beverley KI (1973) The dissociation of sideways movements in depth: psychophysics. *Vision Res* 13, 2403-15.



34. Beverley KI & Regan D (1973) Evidence for the existence of neural mechanisms selectively sensitive to the direction of movement in space. *J Physiol* 235, 17-29.
- 34a. Beverley KI & Regan D (1973) Selective adaptation in stereoscopic depth perception. *J Physiol* 232, 40-41P.
35. Regan D & Beverley KI (1973) Relation between the magnitude of flicker sensation and evoked potential amplitude in man. *Perception* 2, 61-5.
36. Regan D & Beverley KI (1973) Electrophysiological evidence for the existence of neurones sensitive to the direction of depth movement. *Nature* 246, 504-6.
37. Richards W & Regan D (1973) A stereo field map with implications for disparity processing. *Invest Ophthalmol* 12, 904-9.
38. Cartwright RF & Regan D (1974) Semi-automatic, multi-channel Fourier analyser for evoked potential analysis. *Electroenceph clin Neurophysiol* 36, 547-50.
39. Regan D (1974) Electrophysiological evidence for colour channels in human pattern vision. *Nature* 250, 437-49.
40. Regan D & Spekreijse H (1974) Evoked potential indications of colour blindness. *Vision Res* 14, 89-95.
41. Heron JR, Regan D & Milner BA (1974) Delay in visual perception in unilateral optic atrophy after retrobulbar neuritis. *Brain* 97, 69-78.
42. Beverley KI & Regan D (1974) Temporal integration of disparity information in stereoscopic perception. *Exp Brain Res* 19, 228-32.
43. Beverley KI & Regan D (1974) Visual sensitivity to disparity pulses: evidence for directional selectivity. *Vision Res* 14, 357-61.
44. Regan D (1974) Visually evoked potential methods with clinical application. *Proc 11th ISCERG Symp, Bad Neuheim (1973). Docum Ophthal Proc Series* 4, 285-301.
45. Milner BA, Regan D & Heron JR (1974) Differential diagnosis of multiple sclerosis by visual evoked potential recording. *Brain* 97, 755-72.
46. Regan D (1975) Colour coding of pattern responses in man investigated by evoked potential feedback and direct plot techniques. *Vision Res* 15, 175-83.
47. Heron JR, Milner BA & Regan D (1975) Measurement of acuity variations within the central visual field caused by neurological lesions. *J Neurol Neurosurg Psychiat* 38, 356-62.
48. Regan D, Schellart NAM, Spekreijse H & van den Berg TJTP (1975) Photometry in goldfish by electrophysiological recording. *Vision Res* 15, 799-807.
49. Beverley KI & Regan D (1975) The relation between discrimination and sensitivity in the perception of motion in depth. *J Physiol* 249, 387-98.
50. Regan D (1975) Recent advances in electrical recording from the human brain. *Nature* 253, 401-7.
51. Regan D, Milner BA & Heron JR (1976) Delayed visual perception and delayed visual evoked potentials in the spinal form of multiple sclerosis and in retrobulbar neuritis. *Brain* 99, 43-66.
52. Regan D, Varney P, Purdy J & Kraty N (1976) Visual field analyser: assessment of delay and temporal resolution of vision. *Med Biol Engng* 14, 8-14.
53. Regan D (1976) Latencies of evoked potentials to flicker and to pattern speedily estimated by simultaneous stimulation method. *Electroenceph clin Neurophysiol* 40, 654-60.



54. Galvin RJ, Regan D & Heron JR (1976) A possible means of monitoring the progress of demyelination in multiple sclerosis: effect of body temperature on visual perception of double light flashes. *J Neurol Neurosurg Psychiat* 39, 861-5.
55. Galvin RJ, Regan D & Heron JR (1976) Impaired temporal resolution of vision after acute retrobulbar neuritis. *Brain* 99, 255-68.
56. Regan D (1977) Fourier analysis of evoked potentials: some methods based on Fourier analysis. In JE Desmedt (Ed), *Visual evoked potentials in man: new developments*. Oxford: Oxford Univ Press, 110-7.
57. Regan D (1977) Rapid methods for refracting the eye and for assessing visual acuity in amblyopia, using steady-state visual evoked potentials. In JE Desmedt (Ed), *Visual evoked potentials in man: new developments*. Oxford: Oxford Univ Press, 418-26.
58. Regan D (1977) Evoked potential indications of the processing of pattern, colour, and depth information. In JE Desmedt (Ed), *Visual evoked potentials in man: new developments*. Oxford: Oxford Univ Press, 234-49.
59. Regan D, Milner BA & Heron JR (1977) Slowing of visual signals in multiple sclerosis, measured psychophysically and by steady-state evoked potentials. In JE Desmedt (Ed), *Visual evoked potentials in man: new developments*. Oxford: Oxford Univ Press, 461-9.
60. Regan D (1977) Speedy assessment of visual acuity in amblyopia by the evoked potential method. *Ophthalmologica* 175, 159-64.
61. Regan D & Spekreijse H (1977) Auditory-visual interactions and the correspondence between perceived auditory space and perceived visual space. *Perception* 6, 133-8.
62. Galvin RJ, Heron JR & Regan D (1977) Subclinical optic neuropathy in multiple sclerosis. *Arch Neurol* 34, 666-70.
63. Regan D (1977) Steady state evoked potentials. *Proc Symp Electrophysiological Techniques in Man*. *J Opt Soc Am* 67, 1475-89.
64. Regan D & Milner BA (1978) Objective perimetry by evoked potential recording: limitations. *Electroenceph clin Neurophysiol* 44, 393-7.
65. Regan D, Silver R & Murray TJ (1977) Visual acuity and contrast sensitivity in multiple sclerosis: hidden visual loss. *Brain* 100, 563-79.
66. Regan D & Beverley KI (1978) Looming detectors in the human visual pathway. *Vision Res* 18, 415-21.
67. Cynader M & Regan D (1978) Neurones in cat parastriate cortex sensitive to the direction of motion in three-dimensional space. *J Physiol* 274, 549-69.
68. Regan D & Beverley KI (1978) Illusory motion in depth: aftereffect of adaptation to changing size. *Vision Res* 18, 209-12.
69. Hillyard SA, Picton TW & Regan D (1978) Sensation, perception and attention: analysis using ERPs. In E Callaway, P Tueting & SH Koslow (Eds), *Event-related brain potentials in man*. New York: Academic, 223-321.
70. Regan D (1978) Assessment of visual acuity by evoked potential recording: ambiguity caused by temporal dependence of spatial frequency selectivity. *Vision Res* 18, 439-45.
71. Regan D, Murray TJ & Silver R (1977) Effect of body temperature on visual evoked potential delay and visual perception in multiple sclerosis. *J Neurol Neurosurg Psychiat* 40, 1083-91.



72. Arden GB, Bodis-Wollner I, Halliday AM, Jeffreys A, Kulikowski JJ, Spekreijse H & Regan D (1977) Methodology of patterned visual stimulation. In JE Desmedt (Ed), Visual evoked potentials in man: new developments. Oxford: Oxford Univ Press, 3-15.
73. Regan D (1978) Investigations of normal and defective colour vision by evoked potential recording. *Mod Probl Ophthal* 19, 19-28.
74. Regan D (1977) Visual evoked potentials and visual perception in multiple sclerosis. *Proc San Diego Biomed Symp*, Vol 16. New York: Academic, 87-95.
75. Regan D (1977) New methods for neurological assessment: overview. *Proc San Diego Biomed Symp*, Vol 16. New York: Academic, 55-62.
76. Regan D, Beverley KI & Cynader M (1978) Stereoscopic depth channels for position and for motion. In SJ Cool & EL Smith (Eds), *Frontiers in visual science*. New York: Springer, 351-72.
77. Regan D (1977) Evoked potentials in basic and clinical research. In A Rémond (Ed), *EEG informatics: a didactic review of methods and applications of EEG data processing*. Amsterdam: Elsevier, 319-46.
78. Regan D (1977) Colour and contrast. In H Spekreijse & LH van der Tweel (Eds), *Spatial contrast: report of a workshop*. Publ for Netherlands Royal Academy of Sciences. Amsterdam: North-Holland, 75-9.
79. Regan D, Beverley KI & Cynader M (1979) Stereoscopic subsystems for position in depth and for motion in depth. *Proc R Soc Lond B* 204, 485-501.
80. Regan D & Tansley BW (1979) Selective adaptation to frequency-modulated tones: evidence for an information-processing channel selectively sensitive to frequency changes. *J Acoust Soc Am* 65, 1249-57.
81. Regan D & Beverley KI (1979) Visually-guided locomotion: psychophysical evidence for a neural mechanism sensitive to flow patterns. *Science* 205, 311-3.
82. Beverley KI & Regan D (1979) Separable aftereffects of changing-size and motion-in-depth: different neural mechanisms? *Vision Res* 19, 727-32.
83. Beverley KI & Regan D (1979) Visual perception of changing-size: the effect of object size. *Vision Res* 19, 1093-1104.
84. Regan D & Cynader M (1979) Neurons in area 18 of cat visual cortex selectively sensitive to changing size: nonlinear interactions between responses to two edges. *Vision Res* 19, 699-711.
85. Regan D (1980) New visual tests in multiple sclerosis. In HS Thompson (Ed), *Topics in neuro-ophthalmology*. Baltimore: Williams & Wilkins, 219-42.
86. Regan D & Beverley KI (1979) Binocular and monocular stimuli for motion-in-depth: changing-disparity and changing-size inputs feed the same motion-in-depth stage. *Vision Res* 19, 1331-42.
87. Regan D, Beverley KI & Cynader M (1979) The visual perception of motion in depth. *Scient Am* 241, 136-51.
88. Regan D (1980) Detection and quantification of neuroophthalmological abnormalities using psychophysical measures of visual delay and temporal resolution. In S Sokol (Ed), *Electrophysiology and psychophysics: their use in ophthalmic diagnosis*. Intl Ophthal Clinics. Boston: Little, Brown, 185-204.



89. Regan D (1981) Visual psychophysical tests in multiple sclerosis as an aid to diagnosis, localization of pathology, and assessment of experimental therapy. In *Clinical applications of visual psychophysics (Proc NAS/NRC Symp)*. New York: Cambridge Univ Press.
90. Tansley BW, Regan D & Suffield JB (1982) Measurement of the sensitivities of information processing channels for frequency change and for amplitude change by a titration method. *Can J Psychol* 36, 723-30.
91. Beverley KI & Regan D (1980) Visual sensitivity to the shape and size of a moving object: implications for models of object perception. *Perception* 9, 151-60.
92. Regan D, Whitlock J, Murray TJ & Beverley KI (1980) Orientation-specific losses of contrast sensitivity in multiple sclerosis. *Invest Ophthalmol Vis Sci* 19, 324-8.
93. Regan D & Beverley KI (1980) Visual responses to changing size and to sideways motion for different directions of motion in depth: linearization of visual responses. *J Opt Soc Am* 11, 1289-96.
94. Regan D (1980) Control system and physiological monitoring applications of steady-state evoked potentials. In FE Gomer (Ed), *Biocybernetic applications for military systems*. DARPA Conf, Chicago (1978). St Louis: McDonnell-Douglas. Report MDC E2191, 175-202.
95. Tansley BW & Regan D (1979) Separate auditory channels for unidirectional frequency modulation and unidirectional amplitude modulation. *Sensory Proc* 3, 132-40.
96. Regan D & Beverley KI (1981) Motion sensitivity measured by a psychophysical linearizing technique. *J Opt Soc Am* 71, 958-65.
97. Regan D (1979) Electrical responses evoked from the human brain. *Scient Am* 241, 134-46.
98. Beverley KI & Regan D (1980) Device for measuring the precision of eye-hand coordination when tracking changing size. *Aviat Space Environ Med* 51, 688-93.
99. Raymond J, Regan D & Murray TJ (1981) Abnormal adaptation of visual contrast sensitivity in multiple sclerosis patients. *Can J Neurol Sci* 8, 221-34.
100. Noseworthy J, Miller J, Murray TJ & Regan D (1981) Auditory brainstem responses in postconcussion syndrome. *Arch Neurol* 38, 275-8.
101. Regan D, Raymond J, Ginsburg A & Murray TJ (1981) Contrast sensitivity, visual acuity and the discrimination of Snellen letters in multiple sclerosis. *Brain* 104, 333-50.
102. Regan D (1980) Speedy evoked potential methods for assessing vision in normal and amblyopic eyes: pros and cons. *Vision Res* 20, 265-9.
103. Petersik JT, Beverley KI & Regan D (1981) Contrast sensitivity of the changing-size channel. *Vision Res* 21, 829-32.
104. Regan D (1984) Chapters 11 & 12 in E Donchin (Ed), *Cognitive psychophysiology*. Hillsdale, NJ: Erlbaum, 303-38.
105. Beverley KI & Regan D (1980) Temporal selectivity of changing-size channels. *J Opt Soc Am* 11, 1375-7.
106. Beverley KI & Regan D (1982) Adaptation to incomplete flow patterns: no evidence for "filling in" the perception of flow patterns. *Perception* 11, 275-8.
107. Regan D (1981) Evoked potential studies of visual perception. *Can J Psychol* 35, 77-112.
108. Cynader M & Regan D (1982) Neurons in cat visual cortex tuned to the direction of motion in depth: effect of positional disparity. *Vision Res* 22, 967-82.
109. Regan D & Cynader M (1982) Neurons in cat visual cortex tuned to the direction of motion in depth: effect of stimulus speed. *Invest Ophthalmol Vis Sci* 22, 535-50.



110. Regan D (1981) Electrophysiology and psychophysics of motion in depth. Proc 18th ISCERG Symp, Amsterdam (1981). Docum Ophthal Proc Series 27, 271-81.
111. Regan D, Regal DM & Tibbles JAR (1982) Evoked potentials during recovery from blindness recorded serially from an infant and his normally sighted twin. *Electroenceph clin Neurophysiol* 54, 465-8.
112. Regan D (1982) Visual information channeling in normal and disordered vision. *Psychol Rev* 89, 407-44.
113. Regan D (1981) Psychophysical tests of vision and hearing in patients with multiple sclerosis. In SG Waxman & JM Ritchie (Eds), *Demyelinating disease: basic and clinical electrophysiology*. Proc Vail Conf MS Soc of USA. New York: Raven, 217-37.
114. Kruk R, Regan D, Beverley KI & Longridge T (1981) Correlations between visual test results and flying performance on the Advanced Simulator for Pilot Training (ASPT). *Aviat Space Environ Med* 52, 455-60.
115. Quine DB, Regan D & Murray TJ (1983) Delayed auditory tone perception in multiple sclerosis. *Can J Neurol Sci* 10, 183-6.
116. Quine DB, Regan D, Beverley KI & Murray TJ (1984) Patients with multiple sclerosis experience hearing loss specifically for shifts of tone frequency. *Arch Neurol* 41, 506-8.
117. Regan D, Kruk R, Beverley KI & Longridge T (1981) The relevance of the channel theory of vision for the design of simulator imagery. Proc Image II conf, Arizona, 307-44.
118. Regan D (1982) Comparison of transient and steady-state methods. *Proc NY Acad Sci* 388, 46-71.
119. Regan D (1986) Binocular vision. In *Encyclopaedia of physics in medicine and biology*. Pergamon, 33-4.
120. Regan D & Beverley KI (1982) How do we avoid confounding the direction we are looking with the direction we are moving? *Science* 215, 194-6.
121. Regan D., Kaufman, L. and Lincoln, J (1986) Motion in depth and visual acceleration. In K.R. Boff, L., Kaufman and J.P. Thomas (Eds.) *Handbook of Perception and Human Performance*, Wiley, New York, p.19-1 to 19-46.
122. Regan D (1987) Human visual evoked potentials. In T Picton (Ed), *Human event-related potentials*. Amsterdam: Elsevier, in press.
123. Kruk R, Regan D, Beverley KI & Longridge T (1983) Flying performance on the Advanced Simulator for Pilot Training and laboratory tests of vision. *Human Factors* 25, 457-66.
124. Regan D (1983) Visual psychophysical tests in demyelinating disease. *Bull Soc Belge Ophtal* 208-I, 303-21.
125. Regan D & Beverley KI (1983) Visual fields described by contrast sensitivity, by acuity and by relative sensitivity to different orientations. *Invest Ophthalmol Vis Sci* 24, 754-9.
126. Beverley KI & Regan D (1983) Texture changes versus size changes as stimuli for motion in depth. *Vision Res* 23, 1387-1400.
127. Regan D & Beverley KI (1984) Psychophysics of visual flow patterns and motion in depth. In L Spillman & BR Wooten (Eds), *Sensory experience, adaptation and perception*. Hillsdale, NJ: Erlbaum, 215-40.
128. Regan D, Bartol S, Murray TJ & Beverley KI (1982) Spatial frequency discrimination in normal vision and in patients with multiple sclerosis. *Brain* 105, 735-54.



129. Regan D (1983) Spatial frequency mechanisms in human vision investigated by evoked potential recording. *Vision Res* 23, 1401-8.
130. Regan D (1984) Visual psychophysical tests in the diagnosis of multiple sclerosis. In CM Poser (Ed), *The diagnosis of multiple sclerosis*. New York: Thieme-Stratton, 64-75.
131. Regan D (1985) Evoked potentials in diagnosis. In M Swash & C Kennard (Eds), *Scientific basis of clinical neurology*. Edinburgh: Churchill Livingstone.
132. Regan D (1982) Visual sensory aspects of simulators. In W Richards & K Dismukes (Eds), *Vision research for flight simulator*. Washington: National Academy Press, 65-71.
133. Regan D & Beverley KI (1983) Visual fields for frontal plane motion and for changing size. *Vision Res* 23, 673-6.
134. Quine DB, Regan D & Murray TJ (1984) Degraded discrimination between speech-like sounds in multiple sclerosis and in Friedreich's ataxia. *Brain* 107, 1113-22.
135. Kruk R & Regan D (1983) Visual test results compared with flying performance in telemetry-tracked aircraft. *Aviat Space Environ Med* 54, 906-11.
136. Regan D (1984) Visual factors in flying performance. *Proc TARP, NAMRL Monograph* 33, 3-10.
137. Regan D, Beverley KI & Macpherson H (1984) Pattern visual evoked potentials in amblyopic children. In R.H. Nodar and C. Barber (Eds.) *Evoked Potentials II*, Butterworth, Boston, pp. 293-301.
138. Regan D (1984). Spatial vision: VEP evidence for mechanisms tuned to spatial frequency. In R.H. Nodar and C. Barber (Eds.) *Evoked Potentials II*. Butterworth, Boston, pp.287-289.
139. Regan D & Beverley KI (1984) Figure-ground segregation by motion contrast and by luminance contrast. *J Opt Soc Am* 1, 433-42.
140. Regan D & Beverley KI (1983) Spatial frequency discrimination and detection: comparison of postadaptation thresholds. *J Opt Soc Am* 73, 1684-90.
141. Regan D & Neima D (1983) Low-contrast letter charts as a test of visual function. *Ophthalmology* 90, 1192-1200.
142. Neima D & Regan D (1984) Pattern visual evoked potentials and spatial vision in retrobulbar neuritis and multiple sclerosis. *Arch Neurol* 41, 198-201.
143. Neima D, LeBlanc R & Regan D (1984) Visual field defects in ocular hypertension and glaucoma. *Arch Ophthalmol* 102, 1042-5.
144. Regan D & Neima D (1984) Visual fatigue and VEPs in multiple sclerosis, glaucoma, ocular hypertension and Parkinson's disease. *J Neurol Neurosurg Psychiat* 47, 673-8.
145. Wilson HR & Regan D (1984) Spatial frequency adaptation and grating discrimination predictions of a line element model. *J Opt Soc Am A* 1, 1091-6.
146. Regan D & Neima D (1984) The balance between pattern and flicker sensitivities in the visual fields of ophthalmological patients. *Br J Ophthalmol* 68, 310-5.
147. Regan D & Beverley KI (1985) Visual responses to vorticity and the neural analysis of optic flow. *J Opt Soc Am A* 2, 280-3.
148. Burbeck CA & Regan D (1983) Independence of orientation and size in spatial discriminations. *J Opt Soc Am* 73, 1691-4.
149. Regan D (1987) Evoked potentials and color-defined categories. In S Harnad (Ed), *Categorical perception*. New York: Cambridge Univ Press, 443-51.



150. Regan D (1985) Evoked potentials and their application to neuro-ophthalmology. *Neuro-ophthalmology* 5, 73-108.
151. Regan D & Beverley KI (1985) Postadaptation orientation discrimination. *J Opt Soc Am A* 2, 147-55.
152. Regan D & Neima D (1984) Low contrast letter charts in early diabetic retinopathy, ocular hypertension, glaucoma and Parkinson's disease. *Br J Ophthalmol* 68, 885-9.
153. Regan D (1985) Masking of spatial frequency discrimination. *J Opt Soc Am A* 2, 1153-9.
154. Spekreijse H, Dangelie G, Maier J & Regan D (1985) Flicker and movement constituents of the pattern reversal response. *Vision Res* 25, 1297-1304.
155. Regan D (1985) New visual sensory tests in neurology and ophthalmology. In A Starr (Ed), *Proc 7th evoked potential workshop*, Univ of California, Irvine (1984). Milan: Amplifon, 101-19.
156. Regan D (1986) Visual processing of four kinds of visual motion. Workshop on "Systems Approach in Vision", Royal Society of the Netherlands 1984, in honour of LH van der Tweel. *Vision Res* 26, 127-45.
157. Regan D (1985) Storage of spatial-frequency information and spatial-frequency discrimination. *J Opt Soc Am A* 2, 619-21.
158. Regan D, Collewijn H & Erkelens CJ (1986) Necessary conditions for motion in depth perception. *Invest Ophthalmol Vis Sci* 27, 584-97.
159. Regan D, Erkelens CJ & Collewijn H (1986) Visual field defects for vergence eye movements and for stereomotion perception. *Invest Ophthalmol Vis Sci* 27, 806-19.
160. Regan D (1985) Visual flow and direction of locomotion: Reply. *Science* 227, 1063-5.
161. Regan D & Maxner C (1987) Orientation-selective visual loss in patients with Parkinson's disease. *Brain* 110, 239-71.
162. Regan D & Maxner C (1986) Orientation-dependent loss of pattern sensitivity and flicker sensitivity in multiple sclerosis. *Clin Vision Sci* 1, 1-23.
163. Regan D (1986) Form from motion parallax and form from luminance contrast: vernier discrimination. *Spatial Vision* 1, 305-18.
164. Morgan MJ & Regan D (1987) Opponent model for line interval discrimination: interval and vernier performance compared. *Vision Res* 27, 107-18.
165. Erkelens CJ & Regan D (1986) Ocular vergence movements induced by changing size and disparity. *J Physiol* 379, 145-69.
166. Collewijn H, Erkelens CJ & Regan D (1986) Absolute and relative disparity: a re-evaluation of their significance in perception and oculomotor control. In E Keller & DS Zee (Eds), *Adaptive processes in visual and oculomotor systems*. Pergamon.
167. Regan D & Price P (1986) Periodicity in orientation discrimination and the unconfounding of visual information. *Vision Res* 26, 1299-1302.
168. Regan D & Spekreijse H (1986) Evoked potentials in vision research: 1961-1985. *Vision Res* 26, 1461-80.
169. Regan D & Regan MP (1987) Spatial frequency tuning, orientation tuning and spatial discrimination investigated by nonlinear analysis of pattern evoked potentials. In C. Barber and T. Blum (Eds.) *Evoked Potentials III*, Butterworths, Stoneham M.A.
170. Apkarian P, Tijssen R, Spekreijse H & Regan D (1987) Origin of notches in CSF: optical or neural? *Invest Ophthalmol Vis Sci* 28, 607-12.



171. Regan D & Regan MP (1988) Objective evidence for phase-independent spatial frequency analysis in the human visual pathway. *Vision Res* 28, 187-91.
172. Regan D & Regan MP (1987) Nonlinearity in human visual responses to two-dimensional patterns and a limitation of Fourier methods. *Vision Res* 27, 2181-3.
173. Regan D & Regan MP (1988) The transducer characteristic of hair cells in the human inner ear: a possible objective measure. *Brain Res* 438, 363-5.
174. Regan D (1988) Low contrast letter charts and sinewave grating tests in ophthalmological and neurological disorders. *Clin Vision Sci*, 2, 235-250.
175. Regan D, Frisby J, Poggio G, Schor C & Tyler CW (1989) The perception of stereo depth: cortical mechanisms. In L. Spillman and J.S. Werner (Eds). *The Neurophysiological Foundations of Visual Perception*. Academic Press, in press.
176. Regan D & Regan MP (1987) "Dissecting" the visual and auditory pathways by means of the two-input technique. *Proc Conf on Electric and Magnetic Activity of the Central Nervous System*, Trondheim, Norway. AGARD Conf Proc. 432, 6, 1-9.
177. Regan D & Neima D (1987) Relation between VEP and visual function in lesions of the optic nerve and visual pathway. *Proc Conf on Electric and Magnetic Activity of the Central Nervous System*, Trondheim, Norway. AGARD Conf. Proc. 432, 38, 1-8.
178. Regan D (1986) The eye in ballgames; hitting and catching. *Sport en zien*. Haarlem: De Vrieseborch, 7-32.
179. Regan MP & Regan D (1988) A frequency domain technique for characterizing nonlinearities in biological systems. *J Theoret Biol*, 133, 293-317.
180. Regan D (1989) A brief review of some of the stimuli used to investigate spatiotemporal vision. In D Regan (Ed), *Spatial Vision*. London: Macmillan, in press.
181. Regan D (1989) Spatial vision in multiple sclerosis. In D Regan (Ed), *Spatial Vision*. London: Macmillan, in press.
182. Regan D. (1989) Detection and spatial discriminations for objects defined by colour contrast, binocular disparity and motion parallax. In D. Regan (Ed), *Spatial Vision*. London: Macmillan, in press.
183. Bodis-Wollner I & Regan D (1989) Spatio-temporal contrast vision in Parkinson's disease and MPTP treated monkeys: the role of dopamine. In D Regan (Ed), *Spatial Vision*. London: Macmillan, in press.
184. Regan D (1989) Depth from motion and motion in depth. In D Regan (Ed), *Binocular Vision*. London: Macmillan, in press.
185. Collewijn H, Steinman RM, Erkelens CJ & Regan D (1989) Binocular fusion, stereopsis and stereoacuity with a moving head. In D Regan (Ed.) *Binocular Vision*. London, Macmillan, in press.
186. Regan D (1988) Visual sensory loss in patients with Parkinson's disease. In I Bodis-Wollner, M. Piccolino (Eds), *Dopaminergic Mechanisms in Vision*. *Neurology & Neurobiology* 43. New York: A.R. Liss, pp. 221-226.
187. Regan D (1988) Low-contrast acuity test for paediatric use. *Can J Ophthalmol*, 23, 224-227.
188. Regan D (1989) Orientation discrimination for objects defined by relative motion and objects defined by luminance contrast. *Vision Res* 29, 1389-1400..



189. Regan D (1989) To what extent can visual defects caused by multiple sclerosis be understood in terms of parallel processing? In B Cohen (Ed), *Vision and the Brain: The Organization of the Central Visual System*. New York: Raven, 317-329.
190. Regan D (1989) Acute spatial discriminations and the unconfounding of visual information. In JJ Kulikowski (Ed), *Seeing Contour and Colour*, 333-339.
191. Regan MP & Regan D (1989) Evoked potential investigations of nonlinear processing stages in human spatial vision. In JJ Kulikowski (Ed), *Seeing contour and colour*, 513-518.
192. Regan MP & Regan D (1989) Objective investigation of visual function using a nondestructive zoom-FFT technique for evoked potential analysis. *Can J Neurol Sci.* 16, 168-179.
193. Hong X & Regan D (1989) Visual field defects for unidirectional and oscillatory motion in depth. *Vision Research*, 29, 809-819.
194. Regan D (1989) Shape discrimination for motion-defined objects. *Perception*, submitted.
195. Regan D & Hong X (1990) Visual acuity for optotypes made visible by relative motion. *Optom. & Vision Science*, in press. (Jan, 1990)
196. Regan D (1989) Magnetic fields generated by the human brain. *Can. Res.* 22, 11-15.
197. Regan D & Hamstra S (1989) Shape discrimination for objects defined by relative motion: effects of presentation duration. *Vision Res* Submitted.
198. Kothe A. & Regan D (1990) Development of visual acuity in children. *Optom & Vision Science*, submitted.
199. Regan D & Regan MP (1989) Ultra-high resolution analysis of auditory and visual brain responses using zoom-FFT. *Proc. 7th Internat. Conf. Biomagnetism*, in press.
200. Regan MP & Regan D (1989) A frequency domain technique for using evoked magnetic fields to test multi-stage models of sensory processing. *Proc. 7th Internat. Conf. Biomagnetism*, in press.
201. Regan D (1989) The relation between shifts of apparent spatial frequency and changes in spatial frequency discrimination caused by adaptation. *Perception*, submitted.
202. Regan D (1989) Do letter charts measure contrast sensitivity? *Clin. Vis. Science*, in press.
203. Regan D & Hong X (1990) Visual resolution, contour interaction and contrast. *J. Opt. Soc. Amer.*, in preparation.
204. Regan MP & Regan D (1990) Nonlinear interactions between visual responses to gratings of different spatial frequencies. *Vision Res.*, in preparation.
205. Regan D, Kothe AC & Sharpe JA (1990) Recognition of motion-defined shapes in patients with multiple sclerosis. *Brain*, in preparation.
206. Kothe AC & Regan D (1990) Crowding in children. *Optom. & Vision Science*, in press.
207. Kothe AC, Regan D and Trope G (1990) Selective disturbance of motion perception in patients with ocular hypertension and glaucoma. *Archiv. Opthal.*, in preparation.
208. Regan D & Hamsta S (1990) Orientation discrimination for motion-defined and contrast-defined bars: temporal integration. *Perception*, in preparation.
209. Regan D (1990) Spatial vision for objects defined by relative motion, color contrast and binocular disparity. *Psych. Review*, in preparation.
210. Regan D (1990) High and low contrast acuity. *Optom. & Vis. Sci.*, in preparation.



PATENTS

Regan, D. & Parr, N. "Improvement in paramedical instrumentation" (Joule-Thomson effect cataract surgery probe). U.K. patent application 4964 (1972). Wilkinson Sword Research."

Regan, D. "Improvements in paramedical instrumentation" (visual acuity measurement). U.K. patent application 4866 (1972). Accepted in U.K., U.S.A., Germany, E. Europe, Japan. Wilkinson Sword Research.

Regan, D. "Improvements in paramedical instrumentation" (multiple sclerosis diagnosis). U.K. patent application 4865(1972). U.S.A. patent N o 3,837,734; West German Patent No 2,304,808. Wilkinson Sword Research.

Regan, D. "Improvements in signal analysis". U.K. patent application 59921 (1972).

Regan, D. "Improved apparatus and methods for optometry" (1972). U.K. patent application 15246/72, 49241/72, 9934/73. U.S.A., E. Europe, W. Germany, U.K. National Research Development Corporation.

Regan, D. "Paramedical apparatus and method" (multiple sclerosis diagnosis). U.K. patent application 25,532 (1964). Wilkinson Sword Research.

Regan D. and Beverley, K.I. "Methods and apparatus for measuring hand-eye coordination while tracking a changing-size image". U.S. patent N o 4,325,697 (1982). U.S. Air Force.

Regan, D. "Paramedical apparatus and method" (eye test chart). U.K. provisional patent 8521775 (1985).



2d. PROFESSIONAL PERSONNEL

D. Regan, Ph.D., D.Sc., F.R.S.C. Professor of Ophthalmology (University of Toronto) and Psychology (York University)

X.H. Hong, Ph.D.

S. Hamstra, M.A.

M.P. Regan, M.Sc.

Joint research was carried out with K. Grasse, Ph.D. (Associate Professor of Psychology, York University)

2e. INTERACTIONS

Papers presented at meetings, conferences, seminars etc.

Formal lectures

The Broadhurst Lecture: "Hyperacuity for objects defined by motion and objects defined by brightness", Eye Research Institute, Boston.

The Association for Research in Vision and Ophthalmology (ARVO) (1989): "Orientation discrimination and shape discrimination for motion-defined targets", D. Regan

The Association for Research in Vision and Ophthalmology (ARVO) (1989): "Motion blindness for unidirectional and oscillatory motion in depth", X. Hong and D. Regan.

The Association for Research in Vision and Ophthalmology (ARVO) (1989): "Nonlinear interactions between responses to different spatial frequencies", M.P. Regan and D. Regan.

Seminars

Wright-Patterson A.F.B.; University of California Berkeley; University of Maryland; Smith-Kettlewell Institute.